Geochimica et Cosmochimica Acta Vol. 52, pp. 1479–1495

0016-7037/88/$3.00 + .00

Ti^{3+} in meteoritic and synthetic hibonite

JOHN R. BECKETT[1], DAVID LIVE[2,3], FUN-DOW TSAY[3], LAWRENCE GROSSMAN[4] and EDWARD STOLPER[1]

[1]Division of Geological and Planetary Sciences, California Institute of Technology, Pasadena, CA 91125, U.S.A.
[2]Department of Chemistry, Emory University, Atlanta, GA 30322, U.S.A.
[3]Jet Propulsion Laboratory, California Institute of Technology, Pasadena, CA 91109, U.S.A.
[4]Department of Geophysical Sciences, University of Chicago, Chicago, IL 60637, U.S.A.

(*Received June* 16, 1987; *accepted in revised form February* 17, 1988)

Abstract—Electron spin resonance has been used to make the first direct determination of Ti^{3+} in synthetic hibonite and hibonite from inclusion SH-7 of the Murchison C2 chondrite. Ti^{3+} concentrations range from 0.02 to 0.64 wt% in synthetic blue hibonite and 0.35–0.44 wt% in hibonite from SH-7. No Ti^{3+} could be detected in orange hibonite, supporting the earlier conclusion that the orange-to-blue transition is associated with the presence of Ti^{3+}. At constant temperature and oxygen fugacity, Ti^{3+}/Ti^{4+} in synthetic hibonite increases with decreasing V but is not strongly dependent on bulk Ti. At the concentration levels encountered in meteoritic hibonite, Fe and Cr contents do not have a significant effect on the amount of Ti^{3+}.

In both synthetic and meteoritic hibonite, Ti^{3+} occupies a 5-coordinated crystallographic site, which is consistent with the formation of doubly ionized oxygen vacancies. At low oxygen fugacities, essentially all Ti^{4+} on the five-fold Al-site has been reduced to Ti^{3+}.

Hibonite from SH-7 equilibrated with a gas that could have been as reducing as a gas of solar composition. This is consistent with other estimates based on mineral equilibria of high temperature oxygen fugacities in Ca-Al-rich inclusions. With the possible exception of Mo-W depletions, indicators based on bulk trace element concentrations in CAIs are inconclusive. There is considerable evidence that as CAIs cooled to lower temperatures, they experienced conditions significantly more oxidizing than those of a solar gas, perhaps in planetary environments.

INTRODUCTION

CONDITIONS IN THE early solar nebula are reflected in the compositions of minerals in Ca-, Al-rich inclusions (CAIs) from chondritic meteorites. There have been several estimates of temperatures (T) of equilibration (ARMSTRONG *et al.*, 1985; STOLPER *et al.*, 1985), cooling rates (STOLPER *et al.*, 1982; STOLPER and PAQUE, 1986) and oxygen fugacity (f_{O_2}) levels (*e.g.*, STOLPER *et al.*, 1982; ARMSTRONG *et al.*, 1985; FEGLEY and PALME, 1985; BECKETT and GROSSMAN, 1986; IHINGER and STOLPER, 1986; KOZUL *et al.*, 1986) experienced by CAIs. The oxygen fugacities recorded by CAIs are of particular interest, since they are sensitive to the composition of the nebular gas, especially proportions of H, C and O. Based on previous studies, variations of many orders of magnitude in oxygen pressures are recorded by CAIs, even within individual inclusions (*e.g.*, ARMSTRONG *et al.*, 1985; FEGLEY and PALME, 1985).

Many oxygen barometers have been constructed for terrestrial rocks based on redox reactions involving Fe^{2+} and Fe^{3+} in minerals (*e.g.*, LINDSLEY, 1976). For CAIs, the use of such oxygen barometers is impractical because of the low concentrations of Fe and the extremely reducing conditions under which CAIs equilibrated. CAIs are, however, often rich in titanium and the ratios of Ti^{3+} to Ti^{4+} in clinopyroxene (STOLPER *et al.*, 1982; BECKETT and GROSSMAN, 1986) and rhönite (BECKETT *et al.*, 1986) have been used as indicators of oxygen fugacity in CAIs that contain these phases. Hibonite is a third phase that may be useful as an oxygen barometer. Meteoritic hibonites contain up to 5 wt% Ti (KEIL and FUCHS, 1971; ALLEN *et al.*, 1978; MACDOUGALL, 1979; ARMSTRONG *et al.*, 1982; MACPHERSON *et al.*, 1983; EL GORESY *et al.*, 1984; MACPHERSON and GROSSMAN, 1984), leading to the possibility that Ti^{3+}/Ti^{4+} can be used to estimate the f_{O_2} levels under which they equilibrated.

In this study, we describe the first direct determination of Ti^{3+} in meteoritic and synthetic hibonite. We have used electron spin resonance (ESR) spectroscopy, a sensitive and widely used technique for the analysis of transition metal ions (*e.g.*, CARRINGTON and MCLAUGHLIN, 1967; ABRAGAM and BLEANEY, 1970), to (a) unequivocally detect Ti^{3+} in hibonite, (b) characterize the site that Ti^{3+} occupies, (c) quantify the concentrations of Ti^{3+} in hibonites, (d) define the relationship between Ti^{3+}/Ti^{4+} in hibonites and f_{O_2}, and (e) estimate the f_{O_2} indicated for hibonite from inclusion SH-7 in Murchison. A preliminary report of the results described here is given in LIVE *et al.* (1986).

SAMPLES

Four synthetic hibonite compositions were examined. Nominal compositions of the oxide mixes are given in Table 1 along with microprobe analyses of hibonite from SH-7. The starting materials were synthesized and described by IHINGER and STOLPER (1986). ALL corresponds to the average composition of orange hibonite from inclusion CG-11 of Allende (ALLEN *et al.*, 1978). The oxide mix for ALL was initially decarbonated and sintered at 1430°C and $\log_{10} f_{O_2} = -11.3$. Bulk composition BA corresponds to that of average core hibonite in the Blue Angel inclusion from Murchison (ARMSTRONG *et al.*, 1982), BA-V is equivalent to BA with no V, and BA-VFC to BA with no V, Fe or Cr. For both BA-V and BA-VFC, sufficient Al_2O_3 was added to the oxide mix in order to maintain hibonite stoichiometry. Oxide mixes for BA, BA-V and BA-VFC were initially decarbonated and sintered at 1430°C and $\log_{10} f_{O_2} = -10.7$, -11.3 and -10.8, respectively.

In addition to the synthetic samples, two samples of hibonite from SH-7 were examined: a single grain (SH-7Hib1) weighing 37 μg and 25 chips (SH-7Hib2) weighing a total of 135 μg. The mineralogy and chemistry of SH-7 are discussed by HASHIMOTO *et al.* (1986). Instrumental neutron activation analysis (INAA) of a 17 μg chip of SH-7 yielded concentrations of 45 ± 20 ppm V (HASHIMOTO *et al.*, 1986) and 4.11 ± 0.16 wt% Ti (L. GROSSMAN, unpublished). The V content determined by INAA for SH-7 is consistent with very low concentrations obtained by microprobe analyses (Table 1). The Ti

TABLE 1. Compositions of synthetic hibonite starting materials and of hibonite from inclusion SH-7 in Murchison

Sample	ALL-2	BA	BA-V	BA-VFC	SH-7*	SH-7Hib1†
Phase	—	—	—	—	Hibonite	Hibonite
CaO	8.4	8.4	8.5	8.5	8.30(.11)§	8.30(.07)
Al_2O_3	79.8	84.1	85.1	85.2	82.73(.41)	87.79(.42)
V_2O_3	0.39	1.1	-	-	0.01(.02)	0.13(.04)
Cr_2O_3	-	0.08	0.06	-	0.03(.02)	0.03(.03)
FeO	0.07	-	0.01	-	0.06(.03)	0.05(.05)
MgO	3.8	2.0	2.0	2.1	2.25(.14)	1.03(.09)
TiO_2‡	7.3	4.1	4.1	4.1	4.90(.22)	2.58(.27)
SiO_2	0.29	0.19	0.18	0.19	0.29(.19)	0.12(.08)
MnO	-	-	-	-	0.02(.02)	0.03(.03)
Sc_2O_3	-	-	-	-	0.11(.06)	n.a.§§
Total	100.1	100.0	100.0	100.1	98.68(.53)	100.06(.48)
Number of Analyses	-	-	-	-	4	14

* Northwestern microprobe; A. Hashimoto, analyst
† Caltech microprobe
§ Numbers in parentheses for an oxide wt % represent one standard deviation computed from the number of analyses for a given phase quoted at the bottom of each column.
‡ All Ti as TiO_2
§§ Not analyzed

concentration determined by INAA is, however, substantially higher than by microprobe analysis, probably due either to higher Ti or to inclusions of perovskite in the INAA sample. From Table 1, it can be seen that the bulk composition of BA-V is similar to the average composition of hibonite in SH-7Hib1, but with higher Ti.

EXPERIMENTAL TECHNIQUES

Analyses of meteoritic melilite and hibonite were obtained on an automated JEOL 733 five-spectrometer electron microprobe at Caltech. All analyses were wavelength dispersive and were obtained at 15 kV using a Faraday cup current of 0.01 μA. Data reduction and ZAF corrections were carried out using the procedure of BENCE and ALBEE (1968) with correction factors calculated using the procedure of PACKWOOD and BROWN (1981) as modified by ARMSTRONG (1984). Analyses of SH-7 samples were also obtained using an automated JEOL 733 five-spectrometer electron microprobe at Northwestern University. All analyses were wavelength dispersive and were obtained at 15 kV using a Faraday cup current of 0.03 μA. Matrix corrections were obtained from the Tracor Northern ZAF program. Standards were well-characterized natural and synthetic minerals and glasses.

ESR spectra were obtained using a Varian E-15 spectrometer operating at 9 GHz at JPL and Varian E-12 and V-4500 spectrometers in the Chemistry department at Caltech operating at 9 and 35 GHz, respectively. All spectrometers used a modulation frequency of 100 kHz. Most spectra were taken at room temperature, but a few spectra were also recorded at temperatures of 4 K–273 K. For each spectrum, one or more sample chips weighing a total of 0.04 to 12 mg were placed in a quartz tube and inserted into the microwave cavity. A powder of the stable free radical compound 2,2-Di(4-tert-octylphenyl)-1-picrylhydrazyl (DPPH; Aldrich) with a single unpaired spin per molecule was used as a standard. The DPPH was diluted to appropriate concentration levels by dispersal in powdered KCl. All spectra were recorded at concentrations well below saturation levels for the ESR spectrometer.

Most of the experimental run products used in this study were produced at 1430°C and $\log_{10} f_{O_2} \geq -12.7$ by IHINGER and STOLPER (1986). This temperature was selected by IHINGER and STOLPER (1986) because it is within the range of hibonite stability in a gas of solar composition (*e.g.*, KORNACKI and FEGLEY, 1984) and because the high temperature promoted rapid equilibration. For the purposes of this study, additional synthesis experiments were performed at $\log_{10} f_{O_2} < -12.7$ at 1430°C and at various oxygen fugacities for temperatures between 901 and 1204°C. Run conditions and experimental results for each bulk composition are given in Table 2. All experiments were conducted in a vertical Deltech VT-31 quench furnace at 1 atm total pressure. Chips of pelletized and pre-sintered starting material were placed in wire cages and suspended in the furnace hot spot at a known temperature and f_{O_2}. Pt wire was used in experiments conducted at 1430°C and $\log_{10} f_{O_2} \geq -12.7$. Ir wire was used for experiments conducted at temperatures below 1400°C and for most experiments with $\log_{10} f_{O_2} < -12.7$ at 1430°C. The temperature was monitored in all experiments by means of a Pt/Pt10Rh thermocouple in a closed-end alumina tube adjacent to the sample. The thermocouple was calibrated against the melting points of Au and Pd. The oxygen fugacity was controlled by a flowing H_2-CO_2 gas mixture and monitored with a Y_2O_3-doped ZrO_2 solid electrolyte ($SIRO_2$) from Ceramic Oxide Fabricators (Eaglehawk, Australia). This sensor was calibrated at the iron-wüstite buffer and in air. For experiments at 901–1204°C and for $\log_{10} f_{O_2} \geq -12.7$ at 1430°C, the sensor was placed in the hot spot adjacent to the sample. For $\log_{10} f_{O_2} < -12.7$ at 1430°C, the sensor was suspended above the hot spot at a lower temperature in order to avoid electronic conduction in the electrolyte under the extremely reducing conditions of the experiments (ETSELL and FLENGAS, 1970). The oxygen fugacity of the experimental gas mixture was measured with the sensor in this configuration at sensor temperatures between 950 and 1200°C (where the electrolyte is a pure ionic conductor) as the temperature of the hot spot was increased to 1430°C. The $\log_{10} f_{O_2}$ of an H_2-CO_2 gas mixture of constant bulk composition is approximately a linear function of $1/T$ (*e.g.*, DEINES *et al.*, 1974). Therefore, the measured $\log_{10} f_{O_2}$'s were plotted as a function of $1/T$. The line so produced was extrapolated to 1430°C to obtain an estimate of $\log_{10} f_{O_2}$ at the hot spot. The uncertainty in $\log_{10} f_{O_2}$ for this procedure is estimated to be ±0.2. For each experiment, the temperature, $\log_{10} f_{O_2}$, run time, quenching medium, color and concentration of Ti^{3+} are given in Table 2. The latter was obtained from ESR measurements described below.

ELECTRON SPIN RESONANCE SPECTROSCOPY (ESR)

When a magnetic field is applied to an unpaired electron, the interaction of the spin of the electron with the magnetic field gives rise to two possible energy levels depending on the orientation of the spin. The energy difference between these two levels of the unpaired spin is $\Delta E = g\mu_B B$, where g is the so-called spectroscopic splitting factor, μ_B a constant called the Bohr magneton and B the applied magnetic field. For a free electron, $g = 2.002$ but the value of g in crystals is generally different due to local crystal field effects and orbital angular momentum. In ESR, a sample containing unpaired electrons is excited by radiation of frequency ν in the microwave region of the electromagnetic spectrum. When the magnetic field is changed such that

$$h\nu = \Delta E = g\mu_B B \quad (1)$$

where h is Planck's constant, a resonance condition is achieved. Unpaired electron spins in the lower energy state are excited into the higher energy level with a consequent absorption of the incident radiation. By integrating over the absorption peak as a function of magnetic field, the number of spins in the sample giving rise to the signal can be determined. In practice, the magnetic field is modulated and the signal is phase-detected with a lock-in amplifier. For typical operating conditions, the output signal is the first derivative of the absorption with respect to magnetic field strength. In order to determine the number of spins giving rise to this ESR signal, the first derivative of the absorption signal is doubly integrated over the magnetic field.

TABLE 2. Experimental run conditions and Ti^{3+} concentrations of synthetic hibonite.

Experiment	T(°C)	$\log_{10} f_{O_2}$	t(hrs)	Quench*	Color†	Wt % Ti^{3+}§	$\log_{10}(Ti^{3+}/Ti^{4+})$◇
BA-1-8	1430	-4.8	10.2	IW	O	<0.01	<-2.39
BA-1-3	1430	-6.5	15.6	W	O	<0.01	<-2.39
BA-1-7	1430	-7.5	27.6	IW	O	0.04	-1.75
BA-2-14	1430	-8.8	23.7	N_2	G	0.06	-1.60
BA-1-6	1430	-10.7	22.4	IW	G	0.13	-1.27
BA-2-51	1430	-15.2	5.3	N_2	B	0.13	-1.25
BA-2-52	1430	-15.2	5.3	N_2	B	0.10	-1.36
BA-2-57	1204	-14.8	47.7	N_2	B	0.05	-1.72
BA-V-9	1430	-6.6	49.9	N_2	B	0.10	-1.36
BA-V-10	1430	-6.6	49.9	N_2	B	0.10	-1.38
BA-V-1	1430	-10.7/-7.5	2.0/19.7	IW	B	0.11	-1.32
BA-V-6	1430	-8.5	23.7	N_2	B	0.17	-1.12
BA-V-0	1430	-11.3	22.4	?	B	0.19	-1.08
BA-V-7	1430	-12.7	16.6	N_2	B	0.17	-1.14
BA-V-51	1430	-15.2	5.3	N_2	B	0.27	-0.91
BA-V-55	1204	-14.8	47.7	N_2	B	0.21	-1.04
BA-V-53	1000	-18.0	63.1	N_2	B	0.26/0.27‡	-0.92
BA-V-52	1000	-18.6	25.8	W	B	0.23	-0.98
BA-V-54	901	-20.1	115.3	N_2	B	0.25	-0.96
BA-VFC-2	1430	-10.8	2.8	atm	B	0.24	-0.96
ALL-2-8	1430	-6.6	49.9	N_2	G	0.07	-1.82
ALL-2-1	1430	-10.7/-7.5	2.0/19.7	IW	B	0.17	-1.41
ALL-2-6	1430	-8.5	23.7	N_2	B	0.21	-1.31
ALL-2-0	1430	-11.3	22.4	?	B	0.52	-0.87
ALL-2-58	1430	-11.8	17.2	N_2	B	0.56	-0.83
ALL-2-7	1430	-12.7	16.6	N_2	B	0.39	-1.01
ALL-2-57	1428	-14.0	23.7	N_2	B	0.54	-0.85
ALL-2-51	1430	-15.2	5.3	N_2	B	0.55/0.55‡	-0.84
ALL-2-56	1204	-14.8	47.7	N_2	B	0.57	-0.83
ALL-2-53	1000	-18.0	63.1	N_2	B	0.62	-0.78
ALL-2-52	1000	-18.6	25.8	W	B	0.40/0.42‡	-1.00
ALL-2-55	901	-20.1	115.3	N_2	B	0.64	-0.77

* Quenching medium. atm: bottom port of furnace under flowing gas; IW: ice-water; W: water; N_2: liquid nitrogen.
† B: blue; G: green; O: orange.
§ One standard deviation in concentrations is 3% relative and 10% absolute.
‡ Wt % Ti^{3+} in bulk / Wt% Ti^{3+} in core sample. See text for explanation.
◇ Ti^{3+} to Ti^{4+} ratios are computed for bulk samples.

Ti^{3+} in synthetic hibonite

A stack of ESR spectra taken at room temperature on synthetic hibonite (BA, BA-V) equilibrated at 1430°C is shown in Fig. 1. Each spectrum represents the first derivative of the absorption with respect to magnetic field plotted against magnetic field for an individual run product. The units of absorption are arbitrary, but all the spectra are normalized to constant operating conditions and constant sample weight. The first derivative of a symmetric absorption peak plots above the baseline on the low magnetic field side where slopes are positive, passes through the baseline at a g-value corresponding to that of the absorption peak and plots below the baseline on the high field side where slopes are negative. In Fig. 1, a signal centered at $g = 1.96$ is seen in samples equilibrated under reducing conditions.

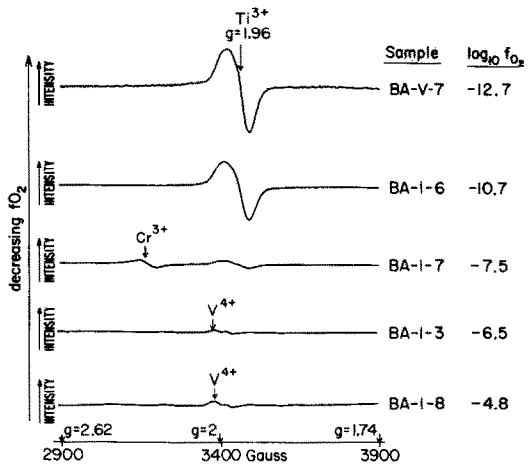

FIG. 1. Stack of ESR spectra of synthetic hibonite spanning a range of oxygen fugacities. Each spectrum shows the first derivative of absorption as a function of magnetic field strength. All spectra were taken at room temperature and a frequency of 9.1 GHz and are normalized to constant sample weight.

The existence of an ESR signal implies that the resonating species has one or more unpaired electrons. Thus, it cannot be due to Ti^{4+}, which has no unpaired electrons. Since the g-value is less than 2, it is consistent with a transition metal ion with a half-filled orbital (*e.g.*, Ti^{3+}, Sc^{2+}, Cr^{5+}; ABRAGAM and BLEANEY, 1970). Several lines of evidence lead to the conclusion that the signal centered at $g = 1.96$ is due to the d^1 ion Ti^{3+}. First, the value of the g-factor in our synthetic hibonites is similar to that reported for Ti^{3+} in octahedral Al-sites of β-alumina (BARRET *et al.*, 1985) and for Ti^{3+} in silicate glasses (*e.g.*, JOHNSTON, 1965; SCHREIBER *et al.*, 1978). Second, the signal centered at $g = 1.96$ is present in the spectrum of BA-VFC, in which Ti is the only transition element, at approximately the same level as for other BA compositions. Third, it can be seen in Fig. 1 that the relative intensity of the signal centered at $g = 1.96$ increases with decreasing oxygen fugacity, consistent with the progressive reduction of Ti^{4+} to Ti^{3+}. This is inconsistent with the occurrence of Cr^{5+}, since this species should occur only under very oxidizing conditions (SCHREIBER and HASKIN, 1976) and the concentration of Cr^{5+} would be expected to decrease, not increase, with oxygen fugacity. Finally, Fe^{2+} and Cr^{3+} are also unlikely

candidates for the prominent feature centered at $g = 1.96$ because the g-values for these species are in excess of 2.2 (O'REILLY and MACIVER, 1962; LOW, 1968).

Under very oxidizing conditions, ESR signals attributable to Cr^{3+} and V^{4+} (*e.g.*, SCHREIBER *et al.*, 1978) are observed. Two examples of this are given in Fig. 1. Intensity of the V^{4+} signal increases with increasing f_{O_2}, consistent with oxidation of V^{3+} to V^{4+}. The absence of a Cr^{3+} signal at both high and low oxygen fugacities may indicate reduction of Cr^{3+} to Cr^{2+} at low oxygen fugacities and oxidation of Cr^{3+} to Cr^{5+} or Cr^{6+} at high oxygen fugacities. It may ultimately be possible to use ESR signals due to Cr^{3+} and/or V^{4+} to set limits on the oxygen fugacities recorded in meteoritic hibonites equilibrated under oxidizing conditions.

It should be noted that there is only one ESR signal centered at $g = 1.96$ for each spectrum shown in Fig. 1. If a resonating species has a nuclear spin I, the ESR signal would be split into a hyperfine structure consisting of $2I + 1$ lines of equal intensity. ^{48}Ti, the most abundant isotope of Ti (87%) has no net nuclear spin ($I = 0$) and hence no hyperfine structure. Hyperfine structure arising from ^{47}Ti ($I = 5/2$) and ^{49}Ti ($I = 7/2$) cannot be seen in our hibonite spectra because of low Ti^{3+} concentrations and line broadening due to the polycrystalline nature of the samples. The lack of hyperfine structure in the hibonite spectra is therefore consistent with a Ti^{3+} signal. On the other hand, virtually all natural V is present as ^{51}V with $I = 7/2$, resulting in our observation of a very well defined hyperfine structure around the V^{4+} signal. Thus, the lack of hyperfine structure in the spectra of synthetic hibonite at $g = 1.96$ eliminates V^{2+} and V^{3+} as a possible candidate.

Ti^{3+} in Murchison hibonite

In Fig. 2, the intensity of the first derivative with respect to magnetic field of the absorption signal for the polycrystalline sample SH-7Hib2 from Murchison is plotted against magnetic field. The units of absorption are arbitrary. The spectrum is characterized by a single ESR signal centered at $g = 1.96$, the apparent structure on the high g side being due to preferred orientation of the chips. The possibility that the signal in SH-7 is due to radiation damage can be rejected because this would result in a signal with g-value essentially equal to that of free electrons (*i.e.*, 2.002; LELL *et al.*, 1966). The chemistry of hibonite in SH-7 also places constraints on

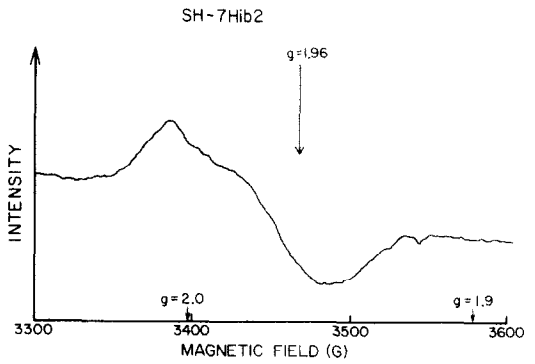

FIG. 2. ESR spectrum taken at room temperature for the collection of chips SH-7Hib2 at a frequency of 9.5 GHz.

the species that generated the ESR signal in Fig. 2. It can be seen in Table 1 that concentrations of transition metal elements other than Ti are very low. By doubly integrating over the absorption peak in Fig. 2, it is found that 2×10^{17} spins are required to generate the observed ESR signal. This is substantially in excess of the total number of spins that could be produced by V^{2+} (2×10^{16}), V^{3+} (3×10^{16}) or Cr^{3+} (6×10^{16}) in this sample.

Given that a similar feature that can be confidently assigned to Ti^{3+} is observed in the ESR spectra of synthetic hibonite samples, these observations support an assignment of the signal centered at $g = 1.96$ in the ESR spectra of natural SH-7 hibonite to Ti^{3+} and argue against any other candidate.

Structural information from ESR spectra

In addition to being used to identify a species, ESR spectra can be used to place constraints on the structural environment of the resonating ion. This information is derived from evaluating the spectra of polycrystalline samples taken at various temperatures and frequencies, and/or evaluating the spectra of single crystals taken at different orientations in the magnetic field.

ESR signals for d^5 or S-state ions (*e.g.*, Mn^{2+}, Fe^{3+}) are readily observed at room temperature regardless of what kind of site the cation occupies. A few other cations can be effectively "S-state" in certain kinds of sites (*e.g.*, Cr^{3+} or V^{2+} in octahedral coordination). Most cations, however, do not have an S-state electronic configuration, and orbital degeneracy leads to short spin-lattice relaxation times and hence line broadening of the ESR signal. For such cations, ESR spectra are observed at room temperature only when the cations are in distorted sites, such as in silicate glasses (*e.g.*, JOHNSTON, 1965; SCHREIBER *et al.*, 1978). The fact that the ESR signal for Ti^{3+} in hibonite is readily observable at room temperature indicates that Ti^{3+} is in a distorted site (ABRAGAM and BLEANEY, 1970; SCHREIBER *et al.*, 1978).

ESR spectra described above were obtained at a frequency of 9 GHz. Better spectral dispersion is obtained by taking ESR spectra at higher magnetic fields and hence higher frequencies. In Fig. 3, an ESR spectrum taken at a frequency of 34.8 GHz is shown for the polycrystalline sample BA-VFC-2. The single ESR resonance centered at $g = 1.96$ (*cf.* Figs. 1, 2), has been resolved into two distinct signals, a consequence of the fact that the g-factor is a tensor property related to site symmetry. The two peaks shown in Fig. 3 indicate an axially symmetric g-tensor that is randomly averaged over all angles due to the polycrystalline nature of the samples. The peak positions correspond to g-values along the principal axes of the g-tensor (*e.g.*, ABRAGAM and BLEANEY, 1970) of $g_{\parallel} = 2.000 \pm 0.002$ and $g_{\perp} = 1.960 \pm 0.002$.

The principal values of the g-tensor can also be obtained by placing a single crystal in various orientations relative to the magnetic field. This was done for SH-7Hib1 by changing the orientation of the magnetic field relative to the cleavage direction of the hibonite crystal. Positions of the ESR signal for SH-7Hib1 relative to the angle between the crystallographic c-axis (assumed to be perpendicular to the cleavage face) and the direction of the magnetic field ($\vec{H}$) are shown in Fig. 4. With rotation through 90°, the resulting sinusoidal curve has a minimum corresponding to $g = 2.001 \pm 0.002$

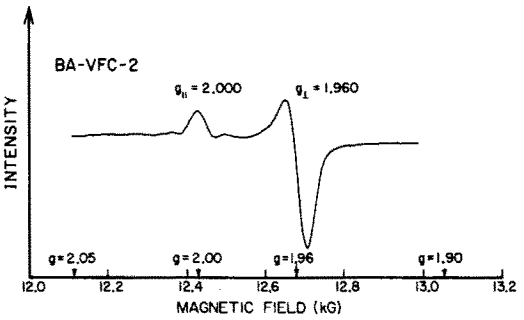

FIG. 3. ESR spectra for BA-VFC-2 taken at room temperature and high frequency (34.8 GHz).

and a maximum corresponding to $g_{\perp} = 1.959 \pm 0.002$. These g-factors agree with those obtained for polycrystalline synthetic hibonite (Fig. 3), implying that Ti^{3+} occupies the same site in meteoritic and synthetic hibonite. From Fig. 4, $g_{\parallel}$ is parallel to the c-axis of hibonite while $g_{\perp}$ is in the ab plane. The only crystallographic site in the hibonite structure that is consistent with this arrangement is the 5-coordinated Al-site (KATO and SAALFELD, 1968; BURNS and BURNS, 1984). Substitution of Ti^{3+} on this particular site is also crystallochemically reasonable. Ti^{3+} has a larger ionic radius than Al (SHANNON and PREWITT, 1969), so it should tend to occupy the largest available position, the 5-coordinated Al-site. This site should also be favored because it is the most distorted of the Al-sites, leading to crystal field stabilization of Ti^{3+} on this Al-site relative to others in the hibonite structure (BURNS, 1970; BURNS and BURNS, 1984). Ti^{4+} also has a larger ionic radius than Al so that some Ti^{4+} may substitute onto the 5-fold Al-site. However, in order to maintain local charge balance, most Ti^{4+} probably substitutes into Al-sites adjacent to those containing Mg. Since Mg probably substitutes into tetrahedral Al-sites (*e.g.*, BETTMAN and PETERS, 1969), most Ti^{4+} is likely to substitute into adjacent octahedral Al-sites and not in the 5-coordinated Al-site (*e.g.*, DYAR *et al.*, 1986).

In spectra of SH-7Hibl and SH-7Hib2 obtained at temperatures as low as 4 K, no signals other than the one centered at $g = 1.96$ were observed. Since ESR signals with g-values of 1.87, 1.91 and 1.97 for Ti^{3+} in symmetric octahedral sites of the structurally similar β-alumina (BRAGG *et al.*, 1931; SATO and HIROTSU, 1976) can be detected at 150 K (BARRET *et al.*, 1985), Ti^{3+} substituting in other Al-sites in hibonite probably would have been observable at low temperatures, if present. We conclude that Ti^{3+} in Murchison hibonite is present dominantly in the 5-coordinated site.

An additional signal at $g = 1.92$ was detected at low temperature in synthetic hibonites BA-VFC-2, ALL-2-51 and BA-V-52 but not observed in the low temperature spectra of BA-V-0 or natural hibonite. The origin of this signal is unclear. It probably does not arise from Ti^{3+} in a crystallographic site of hibonite because no such signal is observed in β-alumina (BARRET *et al.*, 1985). Nor is there a correlation between the presence of this signal and the intensity of the ESR signal centered at $g = 1.96$ or with oxygen fugacity. The signal does not arise from Ti^{3+} in perovskite because the signal is found in samples that do not contain this phase. It is possible that the signal arises from Ti^{3+} on interstitial sites related to the stacking faults that are commonly observed in synthetic hibonite (*e.g.*, SCHMID and DEJONGHE, 1983).

Concentration of Ti^{3+} in hibonite

One of our principal objectives is the quantitative determination of Ti^{3+} concentrations in hibonite based on room temperature ESR measurements. In order to justify this approach, it is necessary to show that there are no contributions to the room temperature ESR signal centered at $g = 1.96$ due to electron-electron interactions, orbital quenching, or Ti^{3+} on other sites. The intensity of an ESR signal arising from Ti^{3+} on one site is proportional to the population difference between the two electron energy levels. This difference is described by the Boltzmann distribution

$$\ln (N_{\alpha}/N_{\beta}) = -(g\mu_B B/k)\left(\frac{1}{T}\right) \qquad (2)$$

where N_{α} and N_{β} are, respectively, the number of spins in the upper and lower energy levels and k is Boltzmann's constant. If there are no complicating factors, the intensity of an ESR signal should vary with inverse temperature in a manner consistent with the Boltzmann distribution. Spectra on the collection of chips SH-7Hib2 and the synthetic hibonite BA-VFC-2 were taken at temperatures as low as 4 K. In Fig. 5, relative peak-to-peak heights of the first derivative ESR signal centered at $g = 1.96$ in the collection of chips SH-7Hib2 are plotted as a function of inverse temperature. All intensities were corrected to constant operating conditions and normalized relative to an intensity of 1.00 for the signal measured at 40 K. In Fig. 5, variations in intensity of the signal centered at $g = 1.96$ in SH-7Hib2 are consistent with the temperature dependence of population differences of electron energy levels for one site. This implies that orbital quenching, electron-electron interactions and contributions from Ti^{3+} on other sites do not contribute significantly to the ESR signal centered at $g = 1.96$. Variations of intensity with inverse temperature for BA-VFC-2 are also consistent with Eqn. (2). We conclude that essentially all Ti^{3+} on crystallographic sites in hibonite was detected and that concentrations of Ti^{3+} may be determined from room temperature ESR measurements.

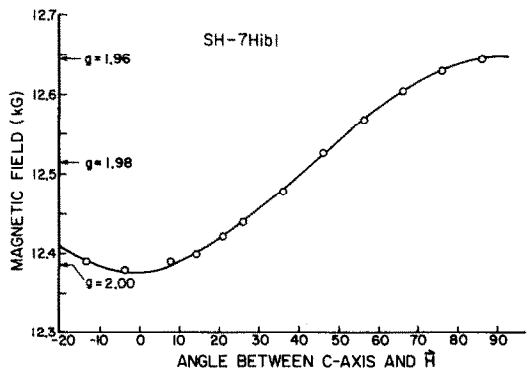

FIG. 4. Values of magnetic field for the single grain SH-7Hibl at the ESR signal centered at $g = 1.96$ as a function of the angle between the crystallographic c-axis and the direction of the magnetic field. Spectra were taken at room temperature at a frequency of 34.8 GHz.

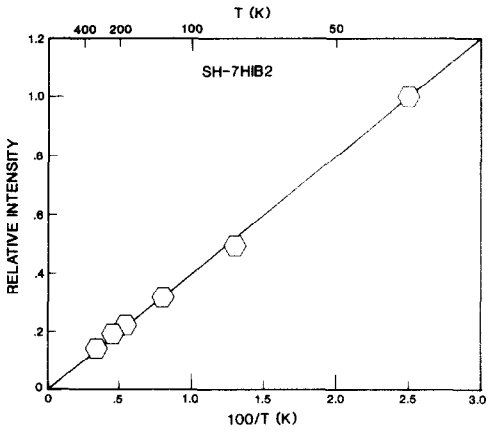

FIG. 5. Relative intensity of signal centered at $g = 1.96$ for SH-7Hib2 as a function of inverse temperature. Points plotting on the line drawn through the origin and the point at 40 K are consistent with a Boltzman distribution for the electron energy level for a single site.

ESR spectra of hibonites were doubly integrated with respect to magnetic field over the signal centered at $g = 1.96$ and normalized to constant operating conditions, DPPH intensity and sample weight to obtain concentrations of Ti^{3+}. Standard deviations on the concentration of Ti^{3+} in a given sample for measurements performed on different days are less than 3% relative. The absolute concentrations of Ti^{3+} given in Table 2 are estimated to be accurate to within 10% based on uncertainties in the relative locations of and differing areas of excitation for sample and standard within the microwave cavity and uncertainties in the baseline used for doubly integrating signal intensity.

Only small concentrations of Ti^{3+} are present in synthetic and meteoritic hibonite. The single grain of hibonite SH-7Hib1 has 0.35 wt% Ti^{3+} after correcting for the presence of ~9 wt% melilite ($X_{Ak} = .01$) and ~1 wt% perovskite in the sample. Thus, 23% of all Ti in the Murchison hibonite SH7-Hib1 is Ti^{3+}. The chips of SH-7Hib2 have an average Ti^{3+} content of 0.44 wt%. The ratio of Ti^{3+} to Ti^{4+} for SH-7Hib2 is uncertain, since the bulk Ti concentration of the chips is unknown. If, however, the chips have an average Ti concentration somewhere between those given for bulk SH-7 and SH-7Hib1 hibonites in Table 2, then 15–28% of all Ti in this sample is Ti^{3+}. Concentrations of Ti^{3+} in synthetic hibonites are given in Table 2. For synthetic blue hibonite, concentrations range from 0.04 to 0.64 wt%, corresponding to 2–15% of Ti as Ti^{3+}. The concentration of Ti^{3+} in orange synthetic hibonite is less than the detection limit (~0.01 wt% Ti^{3+} for those samples). We consider it likely that orange hibonites in meteorites also have essentially no Ti^{3+}.

Concentrations of Ti^{3+} in hibonite can be calculated from electron microprobe analyses (*e.g.*, HAGGERTY, 1978) for an assumed ideal stoichiometry consisting of 13 cations and 19 oxygen anions. For SH-7Hib1, the concentration of Ti^{3+} is calculated from electron microprobe analyses to be 0.60 $\pm$ 0.30 (2σ) wt% in reasonable agreement with the 0.35 wt% determined by ESR. It is concluded below that Ti^{3+}-bearing hibonites are oxygen-deficient relative to the ideal stoichiometry so that recalculated hibonite analyses will generally underestimate the amount of Ti^{3+} that is present. Eighty-one analyses of meteoritic hibonite with total Ti in excess of 1 wt% and for which SiO_2 was also analyzed were obtained from the literature (ALLEN *et al.*, 1978, 1980; MACDOUGALL, 1981; ARMSTRONG *et al.*, 1982; CHRISTOPHE MICHEL-LEVY *et al.*, 1982; BAR-MATTHEWS *et al.*, 1982; MACPHERSON *et al.*, 1983; MACPHERSON and GROSSMAN, 1984; EL GORESY *et al.*, 1984; J. PAQUE, unpublished data; this study). Assuming a stoichiometric formula for hibonite with a total of 13 cations and 19 oxygen anions, the percent of Ti that is Ti^{3+} (*e.g.*, FINGER, 1972) ranges between −25 and +28%. The negative calculated Ti^{3+} is a consequence of analytical errors and underestimation of Ti^{3+} due to oxygen deficiency. Thus, electron probe analyses cannot be used with any confidence to obtain quantitative estimates of Ti^{3+} in hibonite.

OXYGEN FUGACITIES

Effect of hibonite chemistry on Ti^{3+} to Ti^{4+} ratios

In Table 2, $\log_{10}(Ti^{3+}/Ti^{4+})$ for synthetic hibonites equilibrated at 1430°C is given for each bulk composition in order of decreasing oxygen fugacity. For the same oxygen fugacity at 1430°C, Ti^{3+}/Ti^{4+} in BA hibonite is less than that for BA-V hibonite. The only difference between these two bulk compositions is the presence (BA; 1.1 wt% V_2O_3) or absence (BA-V; 0.0 wt% V_2O_3) of a V-component. This implies that Ti^{3+}/Ti^{4+} decreases with increasing V. It is possible that V competes with Ti^{3+} for the 5-coordinated Al-site as proposed by IHINGER and STOLPER (1986). The Ti content of ALL (4.3 wt%) is much higher than that of either BA or BA-V (2.5 wt%). Since the ratio of Ti^{3+} to Ti^{4+} in ALL hibonite is similar to those in BA and BA-V and its V content is intermediate between them, V content is probably more important than bulk Ti in determining Ti^{3+} to Ti^{4+} ratios of hibonite. The fact that the concentrations of Ti^{3+} in BA-VFC-2 and BA-V hibonites equilibrated at about the same oxygen fugacity are similar suggests that the small amounts of Cr and Fe in synthetic and meteoritic hibonite do not significantly affect the concentration of Ti^{3+}.

Under oxidizing conditions ($-10.7 \leq \log_{10} f_{O_2} \leq -6.6$ at 1430°C for BA and BA-V; $-8.5 \leq \log_{10} f_{O_2} \leq -6.6$ for ALL), Ti^{3+} to Ti^{4+} ratios are negatively correlated with f_{O_2} for each composition. Under reducing conditions ($-10.7 \geqslant \log_{10} f_{O_2}$ at 1430°C for BA and BA-V; $-8.5 \geqslant \log_{10} f_{O_2}$ for ALL), Ti^{3+} to Ti^{4+} ratios in synthetic hibonite are approximately independent of f_{O_2} for each composition. Levelling off of Ti^{3+}/Ti^{4+} at the more reducing conditions may be due to reduction of all available Ti^{4+} on the five-fold site, precipitation of other phases in hibonite, and/or difficulties in preserving Ti^{3+} to Ti^{4+} ratios on quenching.

Defect equilibria in synthetic hibonite

Most oxygen barometers are based on reactions that involve the exchange of cations between two or more solid phases (*e.g.*, BUDDINGTON, and LINDSLEY, 1964; EL GORESY and WOERMANN, 1977; SPENCER and LINDSLEY, 1981; EGGLER, 1983; BECKETT and GROSSMAN, 1986). By examining the compositions of coexisting phases, an equilibrium oxygen fugacity can be inferred. Ti^{3+} to Ti^{4+} ratios in individual hi-

bonite crystals provide the basis for a quantitative oxygen barometer, but rather than involving the exchange of Ti^{3+} and Ti^{4+} between condensed phases, the formulation of such an oxygen barometer for hibonite involves homogeneous equilibria in which defects participate.

The vast majority of analyses of meteoritic hibonites shows a nearly 1:1 correlation of Mg:Ti and a 1:−1 correlation of (Ti + Mg):(Al + V + Cr + Sc), suggesting that Mg + Ti substitutes for two trivalent cations (ALLEN *et al.*, 1978). Most Ti in hibonite is, therefore, Ti^{4+} charge-balanced by Mg. There are two basic possibilities for the presence of Ti^{3+} on the 5-coordinated Al-site under reducing conditions. First, Ti^{3+} may substitute directly for Al. Such a Ti^{3+} cation could be oxidized to Ti^{4+} by the formation of cation defects in the hibonite structure (*e.g.*, SCHMID and DE JONGHE, 1983) or by exsolution of a separate phase. Alternatively, Ti^{4+} on the 5-fold site could be reduced to Ti^{3+} by the formation of oxygen vacancies.

The formation of an oxygen vacancy can be described in terms of a reaction between an oxygen anion on a normal site in the crystal and oxygen in a coexisting vapor phase. Thus,

$$O_o = v_o^{\cdot\cdot} + 2e^- + \tfrac{1}{2}O_2 \qquad (3)$$

(*e.g.*, KRÖGER and VINK, 1956; SMYTH, 1976), where O_o represents an oxygen anion in a normal lattice site, $v_o^{\cdot\cdot}$ a doubly ionized oxygen vacancy, and e^- a free electron. In effect, oxygen is removed from the crystal lattice in the process described by reaction (3). If Ti^{4+} is present, then the free electrons created *via* reaction (3) may be trapped by reducing the Ti. Thus

$$Ti^{4+} + e^- = Ti^{3+}. \qquad (4)$$

Equilibrium constant expressions can be written for reactions (3) and (4) as

$$K_1 = \frac{[v_o^{\cdot\cdot}][e^-]^2 f_{O_2}^{1/2}}{[O_o]} \qquad (5a)$$

and

$$K_2 = \frac{[Ti^{3+}]}{[Ti^{4+}][e^-]} \qquad (5b)$$

where the brackets indicate activities (assumed for each Ti species to be equal to its concentration on the five-fold Al-site). For every doubly ionized oxygen vacancy produced in reaction (3), there will be two Ti^{4+} cations reduced *via* reaction (4). Since the number of oxygen vacancies is very small compared to the total number of oxygen anions, $[O_o] \cong 1$. Noting that $[v_o^{\cdot\cdot}] \cong [Ti^{3+}]/2$ and that $[O_o]$ is approximately constant, Eqns. (5a) and (5b) can be rearranged to give

$$\log_{10}\frac{[Ti^{3+}]}{[Ti^{4+}]} + \frac{1}{3}\log_{10}[Ti^{4+}] = A - \frac{1}{6}\log_{10} f_{O_2} \qquad (6)$$

where $A = \frac{1}{3}\log_{10}\{2K_1K_2^2[O_o]\}$ is a constant. It should be emphasized that $[Ti^{3+}]$ and $[Ti^{4+}]$ in Eqn. (6) refer only to concentrations on the five-fold Al-site.

If $[Ti^{3+}] \ll [Ti^{4+}]$ on the five-fold Al site, then $[Ti^{4+}]$ will be approximately constant and Eqn. (6) becomes

$$\log_{10}\frac{[Ti^{3+}]}{[Ti^{4+}]} = A' - \frac{1}{6}\log_{10} f_{O_2} \qquad (7)$$

where $A' = A - (\frac{1}{3})\log_{10}[Ti^{4+}]$ is a constant. Thus, under sufficiently oxidizing conditions, a plot of $\log_{10}([Ti^{3+}]/[Ti^{4+}])$ against $\log_{10} f_{O_2}$ should yield a line with slope of $-\frac{1}{6}$.

In Fig. 6a, $\log_{10}(Ti^{3+}/Ti^{4+})$ in synthetic ALL hibonite equilibrated at 1430°C is plotted as a function of the difference between $\log f_{O_2}^{expt}$ in the experiment and $\log f_{O_2}^{solar}$ for a gas of solar composition. Curves of *bulk* $\log_{10}(Ti^{3+}/Ti^{4+})$ for ALL hibonite were calculated from the bulk Ti concentration (4.38 wt%), using Eqn. (6) to determine $\log_{10}(Ti^{3+}/Ti^{4+})$ on the five-fold Al-site by assuming that the total concentration of Ti on this site is 0.60 wt%, a value approximately equal to the highest measured concentration of Ti^{3+} for this starting material. Most points lie within error of the calculated curve for $A = -2.0$. Under reducing conditions, calculated curves asymptotically approach a bulk $\log_{10}(Ti^{3+}/Ti^{4+})$ corresponding to the ratio of the total concentration of Ti on the five-fold Al-site (0.60 wt% for ALL) to the total concentration of Ti on all other sites (3.78 wt% for ALL). As the amount of Ti on the five-fold Al-site is increased, the limiting Ti^{3+}/Ti^{4+} that is approached as f_{O_2} decreases also increases. Under very oxidizing conditions the curves in Fig. 6a approach slope $-\frac{1}{6}$ lines. In Fig. 6b, a curve calculated using Eqn. (6) is shown for BA assuming that the total amount of Ti on the five-fold Al-site is 0.17 wt% and that $A = -2.0$. Most 1430°C points lie within error of the calculated curve. In Fig. 6c, a curve calculated for BA-V assuming the $A = -2.0$ and the total concentration of Ti on the five-fold Al-site is 0.27 wt%. All but one of the 1430°C data points plot within error of the calculated curve.

As shown in Fig. 6, variations of Ti^{3+}/Ti^{4+} with f_{O_2} for synthetic hibonites can be described in terms of Eqn. (6) using a single value of $A = -2.0$. The principal unknown in the use of Ti^{3+} to Ti^{4+} ratios in hibonites as the basis of an oxygen barometer is the total concentration of Ti on the five-coordinated Al-site. This will depend on the hibonite's composition, especially V-concentration, and may depend on the synthesis conditions. Based on preliminary experiments on ALL hibonite initially synthesized in air but subsequently equilibrated under reducing conditions, the maximum concentration of Ti^{3+} is only 0.4 wt%. This is lower than maximum concentrations of Ti^{3+} (0.6 wt%) measured for ALL initially synthesized under reducing conditions and may indicate a role for initial synthesis conditions on the site occupancy of the five-coordinated Al-site.

Doubly ionized vacancies are the dominant oxygen defect in other oxides (*e.g.*, SMYTH, 1976, 1977; DIRSTINE and ROSA, 1979; TULLER, 1985), so it is reasonable to expect that they are also the dominant defect in hibonite. Data shown in Fig. 6 can, however, be described in terms of neutral or singly ionized oxygen vacancies using expressions analogous to Eqns. (3)–(6). In principle, the dominant type of defect could be distinguished by measurements at high oxygen fugacities where $\log_{10}(Ti^{3+}/Ti^{4+})$ varies with $f_{O_2}^{-1/6}$ for doubly ionized oxygen vacancies, with $f_{O_2}^{-1/4}$ for singly ionized vacancies, and with $f_{O_2}^{-1/2}$ if neutral oxygen vacancies are dominant. Our data do not extend to sufficiently oxidizing conditions for us to make such a distinction, so we cannot reject the possibility of neutral or singly ionized oxygen vacancies. Nevertheless, the consistency of our data with Eqn. (6) and the rarity of neutral and singly ionized oxygen vacancies in

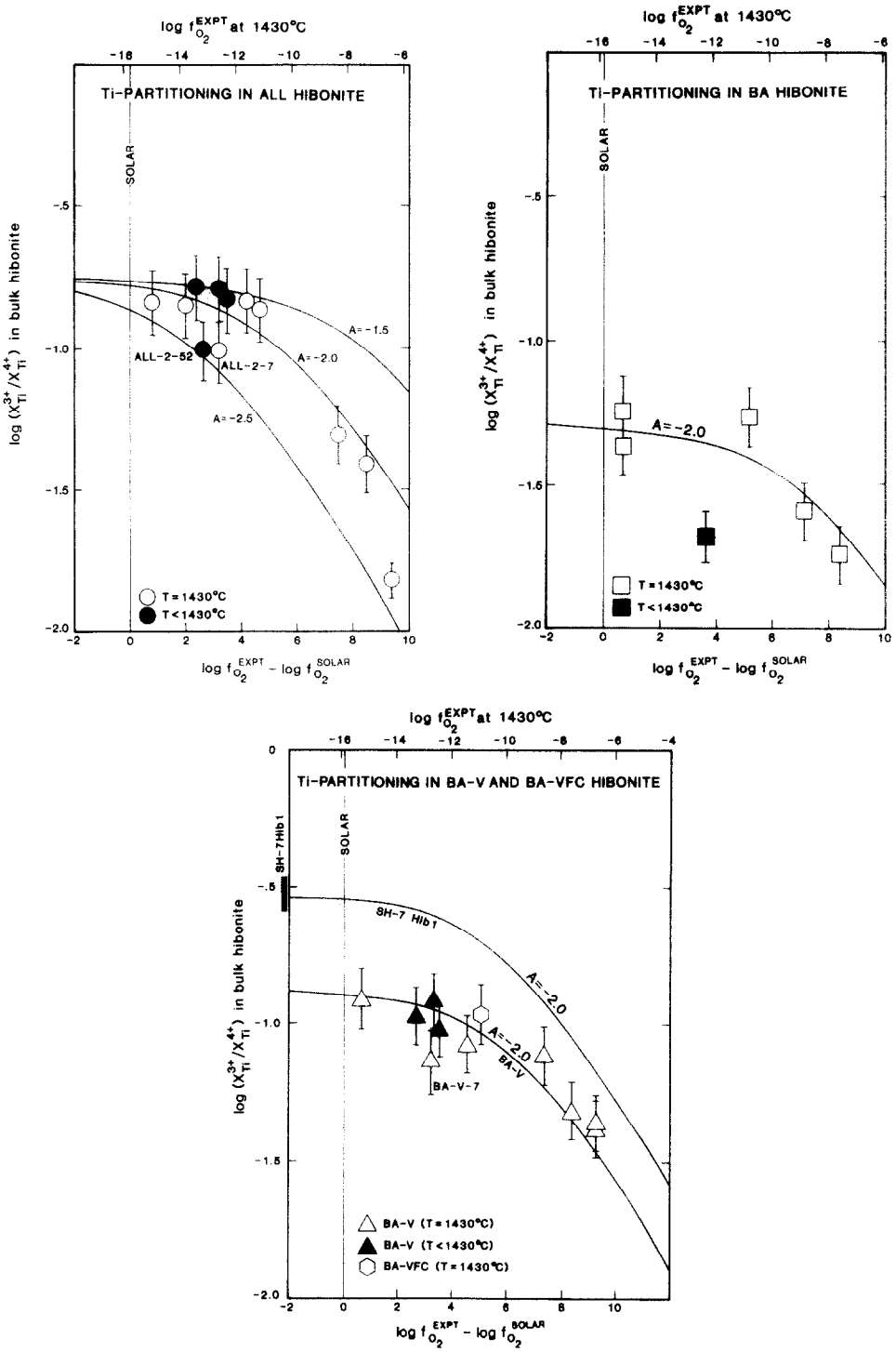

FIG. 6. $Log_{10}(Ti^{3+}/Ti^{4+})$ in synthetic hibonite as a function of the difference in $\log_{10} f_{O_2}$ between that of the experimental gas mix and a gas of solar composition based on H_2/H_2O ratios given in GROSSMAN (1972). Error bars represent a 10% relative error in the concentration of Ti^{3+}. (a) ALL hibonite. Curves of constant A and a concentration of 0.60 wt% Ti on the five-fold Al-site based on Eqn. (6) are shown. (b) BA hibonite. The curve was calculated with Eqn. (6) assuming $A = -2.0$ and that the total concentration of Ti on the five-fold Al-site is 0.17 wt%. (c) BA-V and BA-VFC hibonite. The curve was calculated assuming $A = -2.0$ and that the concentration of Ti on the five-fold Al-site is 0.27 wt%. A curve for SH-7Hib1 is also shown assuming $A = -2.0$ and that the concentration of Ti on the five-fold Al-site is 0.35 wt%. The vertical bar represents the concentration of Ti^{3+} in SH-7Hib1 as determined by ESR.

other systems suggests that doubly ionized vacancies dominate.

Although the saturation in the Ti^{3+} to Ti^{4+} ratio observed at low oxygen fugacities can be readily explained, as we have done in this section, in terms of nearly complete conversion of Ti on the 5-coordinated site to Ti^{3+}, we also considered the possibility that percipitation of other phases under reducing conditions could account for this. Although minor perovskite was observed with an SEM on some of the more reduced samples, it was not present in all of them, and we consider it unlikely that this strongly influences the observed Ti^{3+}/Ti^{4+} relations.

Effects of temperature

The equilibrium oxygen fugacity for a reaction involving O_2 varies as a function of temperature (*e.g.*, BUDDINGTON and LINDSLEY, 1964; EGGLER, 1983; MYERS and EUGSTER, 1983). Hence, in order for Ti^{3+}/Ti^{4+} in hibonite to be useful in constraining oxygen fugacities in natural materials, the dependence of Ti^{3+}/Ti^{4+} on both f_{O_2} *and* temperature must be known. The difference in f_{O_2} between a given pair of redox reactions is often approximately independent of temperature. If this holds for hibonite, then hibonites equilibrated a given number of log units more or less oxidizing than the Ti_2O_3/TiO_2 buffer or a gas of solar composition would have roughly the same Ti^{3+} to Ti^{4+} ratio regardless of temperature. In Fig. 6a, all four hibonites equilibrated at 901–1204°C plot within error of hibonites equilibrated at similar oxygen fugacities relative to solar gas at 1430°C. One sample, ALL-2-52, has a somewhat lower than expected ratio of Ti^{3+} to Ti^{4+}, but it was quenched in water and as discussed below may have reequilibrated on quenching. It was also run for a shorter time than the other low-temperature experiments on ALL and may have failed to reach equilibrium. In Fig. 6c, all the low-temperature data for BA-V plot within error of the calculated curve. In Fig. 6b, the Ti^{3+} to Ti^{4+} ratio for BA-2-57 equilibrated at 1204°C is lower than the expected value based on the 1430°C samples. Since only one low-temperature experiment was conducted on BA, we do not know if it signifies unusual behavior for the sample as a function of temperature, difficulties in achieving equilibrium or larger relative errors at the lower Ti^{3+} concentrations of the BA composition. Although more work needs to be done to establish the details, we conclude that the T-f_{O_2} curve for a gas in equilibrium with a synthetic hibonite of constant composition will approximately parallel that of a gas of solar composition.

Quenching effects

IHINGER and STOLPER (1986) noted that rinds on synthetic hibonite samples are often colored differently from the interiors. They attributed this to quenching effects. To test whether such quenching effects could also contribute to low Ti^{3+}/Ti^{4+} at low f_{O_2}'s in Fig. 6, bulk Ti^{3+} concentrations of three samples (ALL-2-51, ALL-2-52, BA-V-53) originally weighing 4–6 mg were measured. The rinds were then ground off and Ti^{3+} concentrations of the cores (3–5 mg) remeasured. The concentration (Table 2) of Ti^{3+} in the core and bulk sample are within error of each other. Two of these samples were quenched in liquid N_2. The third, ALL-2-52, was quenched in water and has (Fig. 6a) an anomalously low Ti^{3+} to Ti^{4+} relative to other samples equilibrated at similar redox conditions. Thus, quenching in water may result in significant oxidation of hibonite. Two hibonite samples—ALL-2-7 (0.3 mg) and BA-V-7 (0.8 mg)—were much smaller than any others (3–18 mg) used in this study. Their Ti^{3+} to Ti^{4+} ratios are lower (Table 2) than for experiments on the same bulk compositions at either higher or lower oxygen fugacities. Although liquid nitrogen was used, it is likely that these were partially oxidized during quenching.

Origin and intensity of blue color in hibonite

IHINGER and STOLPER (1986) noted that the intensity of color in synthetic blue hibonites increased with decreasing oxygen fugacity. They also found that the intensity of the absorption in the optical spectrum at 715 nm correlated with $\log_{10} f_{O_2}$. In Fig. 7, the intensity of the absorption at 715 nm as given by IHINGER and STOLPER (1986) is plotted against wt% Ti^{3+} determined in this study for the same samples. There is a good correlation, supporting the contention of IHINGER and STOLPER (1986) that intensity of the blue color in hibonite is correlated with the presence of Ti^{3+}. It is possible that the color is due to a transition involving the Ti^{3+} ion. However, since the concentration of oxygen vacancies in hibonite is proportional to the concentration of Ti^{3+}, the blue color could also result from the presence of color centers (see, for example, KITTEL, 1976) caused by oxygen vacancies (BURNS and BURNS, 1984).

Oxygen fugacity for SH-7 hibonite

In Fig. 6c, Ti^{3+}/Ti^{4+} for SH-7Hib1 determined by ESR is shown along with a calculated curve assuming 0.35 wt% Ti on the five-fold Al-site. In this case, the equilibrium oxygen

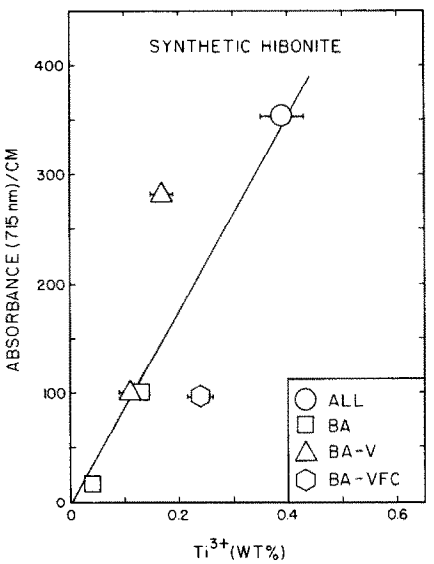

FIG. 7. Absorbance of synthetic hibonite at 715 nm (IHINGER and STOLPER, 1986) as a function of wt% Ti^{3+}. Although normalized to constant thickness (1 cm), optical path lengths for samples are probably variable due to differences in grain size and degree of compactness. In particular, BA-VFC-2 is much less consolidated than are the other samples leading to an anomalously low absorbance.

fugacity for SH-7Hib1 could be as reducing as a gas of solar composition. Alternatively, in the unlikely event that all Ti (1.71 wt%; Table 1) were on the five-fold Al-site in this natural hibonite, then oxygen fugacities approximately nine orders of magnitude more oxidizing than a gas of solar composition are indicated. The correct curve for SH-7Hib1 depends on the unknown concentration of Ti in the 5-fold site. A curve for SH-7Hib2 analogous to the one for SH-7Hib1 in Fig. 6c would be similar, but its position is even less well constrained because the bulk concentration of Ti is not well known. A more quantitative estimate of the equilibrium oxygen fugacity for SH-7 hibonites will be possible only if the site occupancy of Ti^{4+} can be determined. This information could be obtained either from a single crystal structure refinement or by experimentally determining a redox curve similar to those shown in Fig. 6 on a sample of SH-7 hibonite.

It is notable in Fig. 6c that maximum concentrations of 5-coordinated Ti^{3+} in synthetic hibonite are much lower than observed in SH-7Hibl. This could be an artifact of the synthesis procedure. For example, the synthetic hibonite was initially synthesized from oxides and Ca-carbonate under conditions more oxidizing than the TiO_2-Ti_3O_5 buffer using the oxide TiO_2 as a source of Ti. Under these conditions, the Ti substituting on the five-fold Al-site may have been present almost exclusively as Ti^{3+}-$v_o^{\cdot\cdot}$ couples. If SH-7 hibonite grew under conditions more reducing than the TiO_2-Ti_3O_5 buffer, then there may have been a higher concentration of Ti^{3+}-$v_o^{\cdot\cdot}$ couples and, in addition, some Ti^{3+} may have substituted into the five-coordinated site without forming an associated oxygen vacancy. If so, the perovskite frequently observed in meteoritic hibonite (*e.g.*, HASHIMOTO *et al.*, 1986; WARK, 1986) may result from exsolution during oxidation. In conclusion, although we cannot quantify the f_{O_2} under which SH-7 hibonite originally grew, our observations point to conditions more reducing than those used for hibonite synthesis in this study.

COSMOCHEMICAL IMPLICATIONS

Estimates of oxygen fugacity in CAIs range from four orders of magnitude more reducing than a gas of solar composition (STOLPER *et al.*, 1982) to ten orders of magnitude more oxidizing (IHINGER and STOLPER, 1986). This is a tremendous range that cannot be readily explained by exposure of CAIs to a gas with a single composition. There are three basic questions to be addressed. First, is there evidence of multistage processing of individual CAIs, or did each CAI follow a simple T-f_{O_2} path as it cooled? Multistage processing might indicate dynamic and turbulent environments. Second, are there significant differences in T-f_{O_2} histories between individual CAIs within a given class or between CAIs of different classes? This has implications for heterogeneity in the solar nebula. Third, how reducing was the solar nebula at high ($\gtrsim$1100°C) temperatures? Oxidizing conditions could suggest that CAIs evolved from a dust-rich environment (*e.g.*, WOOD, 1984) so that a substantial quantity of preexisting solids were vaporized prior to condensation. Reducing conditions comparable to those of a gas of solar composition would suggest that the region of the solar nebula from which CAIs evolved was initially (before dust vaporization) relatively dust-free. To address these questions, we will review available f_{O_2} estimates in CAIs. Where possible, the relative timing and temperature of equilibration for the f_{O_2} estimate is considered. We begin with those estimates based on properties of individual phases or phase assemblages and then consider constraints based on trace elements in bulk CAIs.

Ti^{3+} to Ti^{4+} ratios

i. Hibonite. In this work, Ti^{3+} to Ti^{4+} ratios of synthetic and meteoritic hibonites have been studied. A lower limit in oxygen fugacity comparable to that of a gas of solar composition has been established for hibonite from inclusion SH-7 in the CM meteorite Murchison. Although a quantitative estimate of equilibrium oxygen fugacity for SH-7 can only be obtained if the site occupancy of Ti can be determined, the high Ti^{3+}/Ti^{4+} of this hibonite relative to our synthetic hibonites suggest highly reducing conditions. Since there are no signs of low-temperature alteration products in this inclusion, the hibonite may record high temperature conditions in the solar nebula.

Based on optical spectroscopy, IHINGER and STOLPER (1986) estimated the f_{O_2} recorded by blue hibonites in the Blue Angel inclusion (ARMSTRONG *et al.*, 1982) of Murchison. They inferred that the hibonite equilibrated in a gas that was four or five orders of magnitude more oxidizing than a gas of solar composition, though this result may also be influenced by details of Ti-site occupancy. The Blue Angel inclusion is especially interesting because it contains a large amount of secondary calcite. This led ARMSTRONG *et al.* (1982) to conclude that the inclusion had been altered under relatively oxidizing conditions in a planetary environment. Since the color (IHINGER and STOLPER, 1986) and Ti^{3+} to Ti^{4+} ratio (this work) of hibonite equilibrate rapidly, it is possible that the oxygen fugacity estimated for the Blue Angel inclusion reflects conditions during the formation of calcite in the inclusion.

STOLPER and IHINGER (1983) showed that orange hibonite in fluffy type A inclusions (MACPHERSON and GROSSMAN, 1984) from Allende (ALLEN *et al.*, 1978) equilibrated in a gas that was at least ten orders of magnitude more oxidizing than a gas of solar composition. Blue hibonites equilibrated in some more reducing environment. Although the blue-to-orange transition does depend somewhat on the composition of the hibonite (STOLPER and IHINGER, 1983), it is clear that orange hibonites equilibrated in environments that were highly oxidizing relative to the oxygen fugacities recorded by hibonites in the Blue Angel or SH-7 inclusions from Murchison.

ii. Fassaite. Ti-rich clinopyroxene in most coarse-grained CAIs crystallized from a melt (*e.g.*, MACPHERSON and GROSSMAN, 1981; MACPHERSON *et al.*, 1984) at temperatures on the order of 1200°C (STOLPER, 1982; STOLPER and PAQUE, 1986). These pyroxenes contain variable amounts of Ti^{3+} and Ti^{4+}, suggesting that they might be useful as indicators of f_{O_2}. In order to obtain a quantitative basis for such an oxygen barometer, STOLPER *et al.* (1982) and BECKETT and GROSSMAN (1986) crystallized clinopyroxene in silicate melts at low f_{O_2} levels. STOLPER *et al.* (1982) obtained a simple linear relationship between $\log_{10}(Ti^{3+}/Ti^{4+})$ in clinopyroxene and $\log_{10} f_{O_2}$ in the coexisting gas. They concluded that clinopyroxene in Allende inclusions crystallized in a gas that was 0–4 orders of magnitude more reducing than a gas of solar composition. BECKETT and GROSSMAN (1986) cali-

brated Ti^{3+}-Ti^{4+} exchange reactions involving clinopyroxene, melilite and spinel. They concluded that oxygen fugacities at the time of initial clinopyroxene crystallization were 1.5 ± 1.1 orders of magnitude more reducing than a gas of solar composition for type B (coarse-grained, pyroxene-rich; GROSSMAN, 1975) inclusions. Calculated oxygen fugacities for different inclusions were within error of each other. The principal implication of both STOLPER *et al.* (1982) and BECKETT and GROSSMAN (1986) is that the melting event to which type B's were subjected took place in a very reducing, approximately solar gas.

iii. Rhönite. Beckett and co-workers calculated oxygen fugacities for compact type A inclusions (coarse-grained, melilite-rich, previously molten; MACPHERSON and GROSSMAN, 1979) from Allende based on experimentally calibrated clinopyroxene-melilite-spinel (BECKETT and GROSSMAN, 1986) and rhönite-clinopyroxene-perovskite-spinel (BECKETT *et al.*, 1986) equilibria. They concluded that the oxygen fugacity approximated that of a gas of solar composition during crystallization of clinopyroxene at temperatures on the order of 1150–1260°C. Estimates of f_{O_2} for different inclusions were within error of each other.

Opaque assemblages

The assemblage Fe-rich alloy-magnetite-hercynite occurs in oxide-sulfide-alloy aggregates called Fremdlinge (EL GORESY *et al.*, 1978) or opaque assemblages (BLUM *et al.*, 1988) in CAIs. ARMSTRONG *et al.* (1985) concluded that this relatively common phase assemblage is stable at about 500–600°C and an f_{O_2} of roughly 10^{-27}, three to seven orders of magnitude more oxidizing than a gas of solar composition in this temperature range. There is some controversy about whether these low temperature conditions were experienced by opaque assemblages prior to their incorporation in CAIs and subsequent melting (*e.g.*, ARMSTRONG *et al.*, 1985) or after high temperature processing under reducing conditions (BLUM *et al.*, 1988).

Scheelite-powellite [$Ca(Mo,W)O_4$] solid solutions are also observed in opaque assemblages (ARMSTRONG *et al.*, 1985; BISCHOFF and PALME, 1986). BISCHOFF and PALME (1986) noted that scheelite is sometimes enclosed in NiFe alloy; this was taken to indicate that the NiFe alloy condensed around preexisting grains of scheelite at high temperatures in the solar nebula. Based on condensation calculations, they concluded that oxygen fugacities in the solar nebula must have been as much as eight orders of magnitude more oxidizing than a gas of solar composition at high (~1600 K) temperatures. However, opaque assemblages may have undergone substantial recrystallization and oxidation at low temperatures after high temperature processing (WARK and WLOTZKA, 1982; BLUM *et al.*, 1988). It is thus possible that Ca(Mo, $W)O_4$ formed during oxidation of opaque assemblages at low temperature rather than at high-temperatures. Its presence would, in this view, be a consequence of the original bulk composition of the opaque assemblage containing it and the conditions to which it was subjected at low temperatures. Since oxidation of the alloy in an opaque assemblage would be accompanied by a large volume increase, many cracks and vugs would form in the alloy and oxide. These could provide convenient nucleation sites for scheelite-powellite solid solutions. If so, the occurrence of scheelite enclosed in NiFe metal would not require preexisting high f_{O_2} conditions at high temperature. The plausibility of volatile Mo and W gas species at low temperatures is discussed below.

In summary, some phase assemblages in opaque assemblages indicate equilibration under oxidizing conditions at low temperatures. If the interpretation of BISCHOFF and PALME (1986) that Ca(Mo, $W)O_4$ formed at high temperatures is correct, then extremely oxidizing conditions during condensation at high temperatures would also be indicated.

Intrinsic oxygen fugacity measurements

KOZUL *et al.* (1986) performed intrinsic f_{O_2} measurements on two type B inclusions. Bulk measurements gave f_{O_2} levels 1–1.5 orders of magnitude more oxidizing than the iron-wüstite buffer, about seven orders of magnitude more oxidizing than a gas of solar composition. Measurements on melilite separates were 2 orders of magnitude more oxidizing than the iron-wüstite buffer. They concluded that the high oxygen fugacities implied by their measurements were indicative of late-stage, low temperature alteration.

Host phases for lithophile refractory trace elements

For solar oxygen fugacities, FEGLEY and KORNACKI (1984) calculated that the lithophile refractory elements Ti, Zr, Hf, U and Ta would condense as alloys with noble metals, rather than as pure oxides, but these elements are not generally observed in the noble metal nuggets of CAIs (*e.g.*, EL GORESY *et al.*, 1979; BLANDER *et al.*, 1980; PALME *et al.*, 1982; ARMSTRONG *et al.*, 1985; MURRELL and BURNETT, 1987). In addition to errors in thermochemical data, FEGLEY and KORNACKI (1984) suggested two possibilities to explain this apparent discrepancy. One possibility is that oxygen fugacities in the primitive solar nebula were three or four orders of magnitude more oxidizing than a gas of solar composition so that oxide phases rather than alloys of these elements were stable. Alternatively, even in a solar gas, these elements may substitute into phases such as perovskite or silicates rather than form pure oxides. Indeed, although baddelyite (ZrO_2) has been reported in CAIs (*e.g.*, EL GORESY *et al.*, 1978; LOVERING *et al.*, 1979), the lithophile refractory elements generally do occur in perovskite (KURAT, 1970; ALLEN *et al.*, 1978; MURRELL and BURNETT, 1987) or dispersed at low concentrations in silicates (MURRELL and BURNETT, 1987). Thus, the behavior of these lithophile refractory elements in CAIs does not at the present time provide firm constraints on oxygen fugacities during CAI genesis.

Trace element concentrations in CAIs

A variety of factors including equilibration temperature (PALME and WLOTZKA, 1976; EKAMBARAM *et al.*, 1984), oxygen fugacity (BOYNTON and CUNNINGHAM, 1981; FEGLEY and PALME, 1985), host phase (GROSSMAN *et al.*, 1977; DAVIS and GROSSMAN, 1979), high-temperature gas-solid fractionation (BOYNTON, 1975), and low-temperature alteration (DAVIS *et al.*, 1978) can affect the abundance patterns of trace elements in CAIs. If the effects of oxygen fugacity can be isolated from those due to other factors, then trace

elements can be used as oxygen barometers. Unfortunately, this is not an easy task. For example, Sr and Ba have similar volatilities in a cooling gas of solar composition so that Ba and Sr should condense at about the same temperature. In a more oxidizing gas Ba becomes more volatile than Sr (BOYNTON and CUNNINGHAM, 1981) so that Sr should condense at a higher temperature than Ba. Thus the presence of negative anomalies of Ba relative to Sr in CAIs might indicate oxidizing conditions, and the absence of such anomalies more reducing conditions. There are, however, at least three problems with such a simple interpretation. First, if a CAI equilibrates with the condensing gas to a sufficiently low temperature, then all the Ba will condense regardless of how oxidizing or reducing the vapor phase might be. Thus the lack of a Ba anomaly does not mean that the gas was very reducing. A second problem is that Ba concentrations in CAIs are uncorrelated with those of Sr, perhaps indicating that these elements condensed in different phases (GROSSMAN *et al.*, 1977). Hence, a negative anomaly in Ba could mean that the host phase for Ba was physically fractionated from the host phase for Sr. Third, relative volatilities of trace elements in a solar gas are generally based on the stability of the pure oxide or metal relative to vapor, or the stability of an ideal solution of that element in some host phase. If solid solutions of the trace elements are strongly nonideal (*e.g.*, BOYNTON, 1978), then relative volatilities can be substantially affected. Hence, negative anomalies in Ba might be indicative of significantly different activity coefficients for Ba and Sr in their host phases. Similar problems are encountered for V and U. Both of these elements become more volatile in oxidizing gases relative to their volatilities in a solar gas (BOYNTON and CUNNINGHAM, 1981), suggesting that they might be useful oxygen barometers. V and U are, however, also rather volatile in a gas of solar composition, so that the negative anomalies sometimes observed for these elements could be due simply to high formation temperatures. We conclude, for most trace elements in most CAIs, that the difficulty in separating the influence of oxygen fugacity from other effects makes them problematic as oxygen barometers. Two possible exceptions that we discuss below are Ce relative to other rare earth elements, and Mo and W relative to other refractory siderophiles.

i. Ce abundances. At oxygen fugacities three to five orders of magnitude more oxidizing than a gas of solar composition, Ce becomes highly volatile relative to other rare earth elements. If REE in CAIs condensed in such a gas, large negative Ce anomalies would be expected (BOYNTON and CUNNINGHAM, 1981, DAVIS *et al.*, 1982; BOYNTON, 1985; FEGLEY, 1986). HAL, a hibonite-rich inclusion (DAVIS *et al.*, 1978, 1982; ALLEN *et al.*, 1980) and C1, a type B CAI (WARK and LOVERING, 1982a), have deep negative Ce anomalies (CONARD, 1976; TANAKA *et al.*, 1979) and may, therefore, have condensed from extremely oxidizing gases. Both inclusions are, however, unusual "FUN" (WASSERBURG *et al.*, 1977) inclusions with large isotopic anomalies in many elements. With rare exceptions (*e.g.*, a small Ce anomaly in a fine-grained inclusion from Efremovka; BOYNTON *et al.*, 1986), there is no evidence for Ce anomalies in "normal" CAIs (*e.g.*, WÄNKE *et al.*, 1974; GROSSMAN and GANAPATHY, 1976a,b; DAVIS *et al.*, 1978; MASON and TAYLOR, 1982; EKAMBARAM *et al.*, 1984). This suggests either that condensation of the REEs in most CAIs took place in relatively reducing gases, or that CAIs equilibrated with the nebular gas to such a low temperature that complete condensation of Ce had occurred.

ii. Mo-W abundances. BLANDER *et al.* (1980) and WARK (1980) noted that Mo and W form gaseous oxides at high temperatures more readily than many other refractory elements in CAIs and therefore depletions in these elements could reflect oxidizing conditions in the solar nebula. FEGLEY and PALME (1985) calculated the composition of metal alloys in equilibrium with gases spanning a range of H_2/H_2O ratios but otherwise solar abundances of the elements. They concluded that Mo-W concentrations in CAIs were established at high temperatures and that CAIs with large Mo and W depletions equilibrated in gases that were three or four orders of magnitude more oxidizing than a gas of solar composition. This conclusion contrasts with some of the data reviewed above that indicate approximately solar oxygen fugacities at high temperatures and, if valid, would suggest that oxygen fugacities were highly variable at high temperature in the solar nebula.

In Fig. 8, W/Os ratios of bulk CAIs from the literature are plotted against Mo/Os. All three elements are normalized to concentrations in CI chondrites. The dashed line joins core and bulk analyses for a type B3 (forsterite-bearing) inclusion (WARK *et al.*, 1987). Calculated ratios for equilibrium between Mo-W containing alloys and the gas of the primitive solar nebula assuming varying H_2/H_2O ratios but otherwise solar abundances of the elements at 1600 K are also shown (FEGLEY and PALME, 1985). Most of the analytical data fall in a band extending from Mo-W enriched to Mo-W depleted compositions; the calculated curve of FEGLEY and PALME (1985) is not a good match to the data. This mismatch does not, however, rule out condensation under oxidizing conditions. Mo and W could be highly nonideal in the condensing alloy, or an important gas species may have been left out of

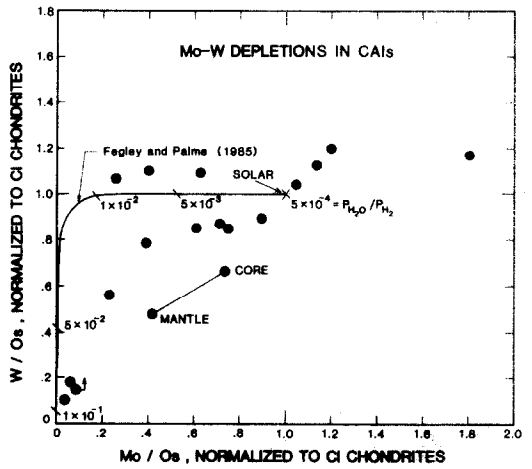

FIG. 8. W/Os as a function of Mo/Os for bulk CAIs. Analyses of the mantle and core of inclusion 818a (WARK *et al.*, 1987) are labeled. The curve shows calculated compositions of alloys in equilibrium with a gas of variable H_2/H_2O ratios but otherwise solar abundances of the elements (FEGLEY and PALME, 1985) at 1600 K. Data were compiled from sources given in FEGLEY and PALME (1985), plus data from EL GORESY *et al.* (1984, 1985), BISCHOFF and PALME (1986), WARK (1986, 1987), and WARK *et al.* (1987).

the calculations. Also, the curve shown in Fig. 8 was calculated for 1600 K. Curves calculated for lower temperatures would more closely approach the observed compositions.

Processes other than condensation in an oxidizing gas might have been responsible for the observed Mo-W depletions. For example, Mo-W depletions could have been established during a melting event (FEGLEY and PALME, 1985). However, some inclusions that never underwent melting (*e.g.*, WARK, 1986) have Mo-W anomalies. Moreover, if Mo and W were volatile during such a melting event, then Ce should also have been volatile. The rarity of Ce anomalies in CAIs argues against such an interpretation. In addition, Ti^{3+}/Ti^{4+} in fassaites from melted inclusions clearly indicate very reducing conditions. Thus, if Mo-W depletions were established during a melting event, they must have occurred before fassaite crystallized. An alternative for the formation of Mo-W depletions is low-temperature oxidation (*e.g.*, PALME *et al.*, 1982). The fact that the mantle of the type B3 inclusion analyzed by WARK *et al.* (1987) is more depleted in Mo and W than the core is consistent with the suggestion that this CAI was immersed in an oxidizing gas after solidification of the inclusion and that Mo and W evaporated into the gas from the outer portions of the inclusion.

Under reducing conditions, W and Mo do not form volatile oxides. In oxidizing, water-rich gases, however, they volatilize to form the gaseous hydroxides $WO_2(OH)_2$ and $MoO_2(OH)_2$ (BELTON and MCCARRON, 1964; BELTON and JORDAN, 1965; SYMONDS *et al.*, 1987) *via* the reactions

$$W_{(s)} + 4H_2O_{(g)} \rightarrow WO_2(OH)_{2(g)} + 3H_{2(g)} \quad (8a)$$

and

$$Mo_{(s)} + 4H_2O_{(g)} \rightarrow MoO_2(OH)_2(g) + 3H_{2(g)}. \quad (8b)$$

If no Mo- or W-bearing phases are stable when reactions (8a, b) occur, then a Mo-W depletion will result. In CAIs, scheelite-powellite and molybdenite (MoS_2)-tungstenite (WS_2) solid solutions are the most frequently observed Mo-W-bearing phases (*e.g.*, EL GORESY *et al.*, 1978; BLANDER *et al.*, 1980; ARMSTRONG *et al.*, 1985). Since Ca is lost from CAIs during the alteration process (WARK, 1981) and $Ca(OH)_2$ is the dominant Ca-bearing species in water-rich nebular gases (HASHIMOTO and WOOD, 1986), scheelite-powellite may condense at low temperatures by means of the reactions

$$WO_2(OH)_{2(g)} + Ca(OH)_{2(g)} = CaWO_{4(s)} + 2H_2O_{(g)} \quad (9a)$$

and

$$MoO_2(OH)_{2(g)} + Ca(OH)_{2(g)} = CaMoO_{4(s)} + 2H_2O_{(g)}. \quad (9b)$$

Similarly, the formation of Mo-W sulfides at low temperatures can be ascribed to reactions of the type

$$WO_2(OH)_{2(g)} + S_{2(g)} = WS_{2(s)} + H_2O_{(g)} + \frac{3}{2}O_{2(g)} \quad (9c)$$

and

$$MoO_2(OH)_{2(g)} + S_{2(g)} = MoS_{2(s)} + H_2O_{(g)} + \frac{3}{2}O_{2(g)}. \quad (9d)$$

For a particular CAI, the specific T-f_{O_2}-f_{H_2O}-f_{S_2} conditions will control whether or not Mo and W become volatile, whether the Mo- and/or W-bearing vapors escape or condense inside the inclusion, and which of reactions (9a–d) is dominant. Note in Fig. 8 that some CAIs have Mo-W enrichments; these can readily occur *via* reactions (9a–d) if Mo-W-bearing vapors escape from one CAI and condense in another at a lower temperature or in a more reducing gas. Subtle variations in physical conditions may thus control whether or not a given inclusion will have a Mo-W depletion. It remains to be seen whether the details of the Mo-W depletions in CAIs can be better accounted for by processes at high or low temperatures. Aspects of this problem that need to be explored include the following: (1) What, if any, relationship is there between the alteration event experienced by many CAIs and the oxidation event that produced opaque assemblages? (2) Do inclusions from CM chondrites, which often contain secondary calcite and phyllosilicate, have Mo-W depletion patterns different from CAIs in CO or CV chondrites which do not contain these phases? (3) If Mo and W were volatilized from CAIs at low temperature, would Re, a volatile element in terrestrial volcanic gases (*e.g.*, SYMONDS *et al.*, 1987), also be volatilized? (4) Would phyllosilicates and/or other hydrated solids be expected in CAIs if gases were sufficiently water-rich to stabilize $MoO_2(OH)_{2(g)}$ and $WO_2(OH)_{2(g)}$?

Summary

Constraints on oxygen fugacity during CAI genesis fall into two broad categories. In the first, homogeneous and heterogeneous equilibria recorded by minerals in the CAIs provide quantitative measures of f_{O_2} and, in some cases, temperature. Ti^{3+} to Ti^{4+} ratios in hibonites and fassaites and phase equilibria of opaque assemblages are examples of this type of constraint. This approach is intrinsically quantitative and depends only on the assumption that an equilibrium state was achieved. In the second category, measured concentrations of various elements in CAIs are compared with those expected from a given scenario for CAI genesis where f_{O_2} is a variable used in modelling. Oxygen fugacity estimates based on Ce and Mo-W depletions fall in this category. This second approach is not as quantitative as the first; it depends on the processes assumed to dominate in the evolution of a particular CAI (*e.g.*, equilibrium *vs.* fractional condensation or evaporation), the assumed temperature and total pressure at which the specified gas-solid fractionation occurred, and the bulk composition of the system (*e.g.*, Mo-W depletions may have been inherited by the gas from which CAIs condensed and thus give no information on the conditions under which CAIs formed). In our view, constraints based on mineral equilibria recorded in CAIs are, in general, to be preferred to those based on bulk chemical characteristics of inclusions because they are less model dependent.

Based on these two types of approaches, several constraints have been established on the oxygen fugacities recorded by CAIs. (1) With few exceptions, indications of oxygen fugacity based on lithophile refractory elements are consistent with high temperature gas-solid equilibration under reducing, approximately solar conditions. The absence of Ce anomalies in most "normal" CAIs is the only semi-quantitative indicator of this; other elements (*e.g.*, Ba *vs.* Sr; U *vs.* V) and details of the host phases of refractory lithophiles are inconclusive, but consistent with reducing conditions. (2) The melting event

that affected most type B and many type A inclusions took place under reducing, approximately solar conditions. This is a firm constraint based on Ti^{3+}/Ti^{4+} in pyroxenes and rhönites. Ti^{3+}/Ti^{4+} in the SH7 hibonite studied here is also consistent with reducing conditions at high temperatures. (3) Many CAIs appear to record highly oxidizing conditions relative to those of a solar gas at low temperatures. Phase equilibria of opaque assemblages, intrinsic f_{O_2} measurements and hibonite colors all either demonstrate or are consistent with this conclusion. Mo-W depletions may indicate oxidizing conditions, but it is not clear at what point in CAI evolution these depletions developed, and in particular whether they formed at high or low temperatures.

Among many possible explanations for the variation of oxygen fugacity during CAI evolution that could account for these observations, we propose the following two as examples. The principal difference between them is in the interpretation of observed Mo-W anomalies in CAIs. We assume the overly simplistic view that most "normal" CAIs record a roughly similar set of processes and thus observations from different CAIs can be linked:

(1) Condensation of all components in CAIs occurred under reducing, approximately solar conditions. Some inclusions were later melted under similarly highly reducing conditions. At low temperatures (~600°C), CAIs were exposed to significantly more oxidizing conditions. There are no definite f_{O_2} constraints between 1200 and 600°C, so the nature of the transition between reducing and oxidizing conditions is unclear, though it could reflect a transition from nebular to planetary environments. This scenario would require that Mo-W depletions and enrichments took place at low temperatures, late in the evolution of CAIs.

(2) CAIs accumulated as mixtures dominated by silicate-lithophile components that formed under reducing conditions with other components that formed under oxidizing conditions and carried the Mo-, W-depleted refractory siderophiles. Some of these mixtures were subsequently melted under reducing conditions imposed either by a surrounding reduced gas or by the predominant reduced component of the CAIs. At a later time, CAIs were exposed to very oxidizing conditions at low temperatures. According to this scenario, Mo-W depletions predate the accumulation and melting of CAIs. They reflect the origin of a minor component in CAIs rather than the evolution of CAIs as bulk objects. It may be that many of the apparent discrepancies among various indicators of oxygen fugacity can be resolved by decoupling the origins of different chemical components in these inclusions prior to their agglomeration into CAIs.

It should be emphasized that although the extreme variations in oxygen fugacity at high temperatures that have been proposed recently for most CAIs (ARMSTRONG *et al.*, 1985; FEGLEY and PALME, 1985; BISCHOFF and PALME, 1986) cannot be ruled out, we find no conclusive evidence for them. While there is certainly evidence in CAIs of multistage processing and variations in gas compositions at high temperatures (*e.g.*, GROSSMAN, 1980; WARK and LOVERING, 1982b; WARK, 1986), available T-f_{O_2} constraints are consistent with the suggestion that most of these processes occurred in very reducing gases. Dust-rich gases invoked by WOOD (1984) to explain anomalously high oxygen fugacities in the solar nebula are not required for the high-temperature histories of CAIs. CAIs, however, may have been exposed to such environments at low temperatures. Alternatively, the oxidized, low temperature environments could have been planetary.

CONCLUSIONS

(1) Electron spin resonance spectroscopy has been used to demonstrate the existence of Ti^{3+} in meteoritic and synthetic hibonite, establish which site the Ti^{3+} is located in and quantify concentrations of Ti^{3+}. By obtaining ESR data on Ti^{3+} in synthetic hibonite covering a range of bulk composition and equilibrated experimentally over a range of oxygen fugacities, it has been possible to calibrate a potentially useful oxygen barometer for Ti^{3+}-bearing hibonite. The Ti^{3+} concentrations correlate well with the intensity of the 715 nm absorption signal for blue hibonite described by IHINGER and STOLPER (1986).

(2) Ti^{3+} in hibonite gives rise to an ESR signal centered at $g = 1.96$, which is readily observable at room temperature. The principal values of the g-tensor are $g_\perp = 1.960 \pm 0.002$ and $g_\parallel = 2.000 \pm 0.002$. Ti^{3+} is in the 5-coordinated Al-sites that are aligned parallel to the crystallographic c-axis.

(3) Concentrations of Ti^{3+} in synthetic blue hibonites are in the range 0.04–0.64 wt%, corresponding to 2–15% of Ti as Ti^{3+} for these samples. Ti^{3+} could not be detected in synthetic orange hibonite. The concentration of Ti^{3+} in two samples of blue hibonite from Murchison inclusion SH-7 were 0.35 in a single grain SH-7Hib1 and 0.44 wt% in a collection of chips, SH-7Hib2. Ti^{3+} comprises 23% of all Ti in SH-7Hib1 hibonite.

(4) The observed variations in Ti^{3+}/Ti^{4+} with f_{O_2} in synthetic hibonite of a given bulk composition can be modelled with a simple treatment of the thermodynamics of Ti^{3+}-Ti^{4+} equilibria in hibonite. Under reducing conditions bulk Ti^{3+} to Ti^{4+} ratios in synthetic hibonites become nearly constant due to reduction of essentially all Ti on the five-fold Al-site. Ti^{3+}/Ti^{4+} in hibonite increases with decreasing V content. The oxygen fugacity calculated for a given Ti^{3+} to Ti^{4+} ratio in hibonite is a function of temperature. However, the T-f_{O_2} curve for a gas in equilibrium with a synthetic hibonite of constant composition approximately parallels that of a gas of solar composition.

(5) Hibonite from Murchison inclusion SH-7 equilibrated with a gas that could have been as reducing as a gas of solar composition. This is consistent with more quantitative estimates of oxygen fugacities at high temperatures based on Ti^{3+}-Ti^{4+} exchange equilibria involving pyroxenes and rhönites in CAIs. The rarity of Ce anomalies in CAIs is also consistent with reducing high temperature environments for the condensation of refractory lithophile elements in CAIs. Other indicators of oxygen fugacity at high temperatures in CAIs are inconclusive, but consistent with reducing conditions.

(6) There is considerable evidence that CAIs experienced conditions significantly more oxidizing than solar gas as they cooled to lower temperatures, perhaps in planetary environments. Mo-W depletions in CAIs could reflect high or low temperature oxidizing conditions: if these depletions record high temperature processing, we suggest that the oxidizing

conditions were experienced only by a minor siderophile element-rich component prior to its incorporation into CAIs, not by bulk CAIs or their lithophile components; if these depletions record low temperature processing, they may predate CAI formation or they could have formed during cooling of bulk CAIs.

Acknowledgements—Discussions with J. D. Blum, B. Fegley, P. D. Ihinger, G. J. MacPherson and G. R. Rossman are gratefully acknowledged. Reviews by J. Hertogen, A. Hofmeister, P. D. Ihinger, M. Johnson, J. Kozul, and D. A. Wark greatly improved the manuscript. A. Hashimoto is thanked for his analyses of SH-7 hibonite on the Northwestern University microprobe. This research was supported by NASA grants NAG 9-105 and NAG 9-54. Part of this work was carried out by D. Live at JPL under contract NAS-7-918 to NASA. D. Live also acknowledges an NRC senior resident research associateship. Caltech Division of Geological and Planetary Sciences Contribution 4553.

Editorial handling: J. Hertogen

REFERENCES

ABRAGAM A. and BLEANEY B. (1970) *Electron Paramagnetic Resonance of Transition Ions.* Oxford, 911p.

ALLEN J. M., GROSSMAN L., DAVIS A. M. and HUTCHEON I. D. (1978) Mineralogy, textures and mode of formation of a hibonite-bearing Allende inclusion. *Proc. Lunar Planet. Sci. Conf. 9th,* 1209–1233.

ALLEN J. M., GROSSMAN L., LEE T. and WASSERBURG G. J. (1980) Mineralogy and petrography of HAL, an isotopically-unusual Allende inclusion. *Geochim. Cosmochim. Acta* **44,** 685–699.

ARMSTRONG J. T. (1984) Quantitative analysis of silicate and oxide minerals: A re-evaluation of ZAF and proposal for new Bence-Albee coefficients. In *Microbeam Analysis/1984* (eds. A. ROMIG and J. I. GOLDSTEIN), pp. 208–212. San Francisco Press.

ARMSTRONG J. T., MEEKER G. P., HUNEKE J. C. and WASSERBURG G. J. (1982) The Blue Angel: I. The mineralogy and petrogenesis of a hibonite inclusion from the Murchison meteorite. *Geochim. Cosmochim. Acta* **46,** 575–595.

ARMSTRONG J. T., EL GORESY A. and WASSERBURG G. J. (1985) Willy: A prize noble Ur-Fremdling—Its history and implications for the formation of Fremdlinge and CAI. *Geochim. Cosmochim. Acta* **49,** 1001–1022.

BAR-MATTHEWS M., HUTCHEON I. D., MACPHERSON G. J. and GROSSMAN L. (1982) A corundum-rich inclusion in the Murchison carbonaceous chondrite. *Geochim. Cosmochim. Acta* **46,** 31–41.

BARRET J. P., GOURIER D. and VIVIEN D. (1985) Influence of titanium impurities on the chemical alteration of β' and β''-alumina in sodium environment. ESR study. *Solid State Ionics* **15,** 127–134.

BECKETT J. R. and GROSSMAN L. (1986) Oxygen fugacities in the solar nebula during crystallization of fassaite in Allende inclusions (abstr.). *Lunar Planet. Sci. XVII,* 36–37.

BECKETT J. R., HAGGERTY S. E. and GROSSMAN L. (1986) Origin of Ti^{3+}-bearing rhönite in Ca-, Al-rich inclusions: An experimental study (abstr.). *Meteoritics* **21,** 332–333.

BELTON G. R. and MCCARRON R. L. (1964) The volatilization of tungsten in the presence of water vapor. *J. Phys. Chem.* **68,** 1852–1856.

BELTON G. R. and JORDAN A. S. (1965) The volatilization of molybdenum in the presence of water vapor. *J. Phys. Chem.* **69,** 2065–2071.

BENCE A. E. and ALBEE A. L. (1968) Empirical correction factors for electron probe microanalysis of silicates and oxides. *J. Geol.* **76,** 382–403.

BETTMAN M. and PETERS C. R. (1969) The crystal structure of $Na_2O \cdot MgO \cdot 5Al_2O_3$ with reference to $Na_2O \cdot 5Al_2O_3$ and other isotypal compounds. *J. Phys. Chem.* **73,** 1774–1780.

BISCHOFF A. and PALME H. (1986) Oxidation of refractory metal assemblages at high temperatures (abstr.). *Lunar Planet. Sci. XVII,* 54–55.

BLANDER M., FUCHS L. H., HOROWITZ C. and LAND R. (1980) Primordial refractory metal particles in the Allende meteorite. *Geochim. Cosmochim. Acta* **44,** 217–223.

BLUM J., WASSERBURG G. J., HUTCHEON I. D., BECKETT J. and STOLPER E. (1988) Domestic origin of opaque assemblages in refractory inclusions in meteorites. *Nature* **331,** 405–409.

BOYNTON W. V. (1975) Fractionation in the solar nebula: Condensation of yttrium and the rare earth elements. *Geochim. Cosmochim. Acta* **39,** 569–584.

BOYNTON W. V. (1978) Fractionation in the solar nebula, II. Condensation of Th, U, Pu and Cm. *Earth Planet. Sci. Lett.* **40,** 63–70.

BOYNTON W. V. (1985) Cosmochemistry of the rare earth elements: meteorite studies. In *Rare Earth Element Geochemistry* (ed. P. HENDERSON), pp. 63–114. Elsevier.

BOYNTON W. V. and CUNNINGHAM C. C. (1981) Condensation of refractory lithophile trace elements in the solar nebula and in supernovae (abstr.). *Lunar Planet. Sci. XII,* 106–108.

BOYNTON W. V., WARK D. A. and ULYANOV A. A. (1986) Trace elements in Efremovka fine-grained inclusion E14: Evidence for high temperature, oxidizing fractionations in the solar nebula (abstr.). *Lunar Planet. Sci. XVII,* 78–79.

BRAGG W. L., GOTTFRIED C. and WEST J. (1931) The structure of β-alumina. *Z. Krist.* **77,** 255–274.

BUDDINGTON A. F. and LINDSLEY D. H. (1964) Iron-titanium oxide minerals and synthetic equivalents. *J. Petrol.* **5,** 310–357.

BURNS R. G. (1970) *Mineralogical Applications of Crystal Field Theory.* Cambridge, 224p.

BURNS R. G. and BURNS V. M. (1984) Crystal chemistry of meteoritic hibonites. *Proc. Lunar Planet. Sci. Conf. 15th; J. Geophys. Res.* **89,** C313–C321.

CARRINGTON A. and MCLAUGHLIN D. (1967) *Introduction to Magnetic Resonance with Applications to Chemistry and Chemical Physics.* Harper & Row, 266p.

CHRISTOPHE MICHEL-LEVY M., KURAT G. and BRANDSTÄTTER F. (1982) A new calcium-aluminate from a refractory inclusion in the Leoville carbonaceous chondrite. *Earth Planet. Sci. Lett.* **61,** 13–22.

CONARD R. (1976) A study of the chemical composition of Ca-Al-rich inclusions from the Allende meteorite. M.S. thesis, Oregon State University, Corvallis, 129p.

DAVIS A. M. and GROSSMAN L. (1979) Condensation and fractionation of rare earths in the solar nebula. *Geochim. Cosmochim. Acta* **43,** 1611–1632.

DAVIS A. M., GROSSMAN L. and ALLEN J. M. (1978) Major and trace element chemistry of separated fragments from a hibonite-bearing inclusion. *Proc. Lunar Planet. Sci. Conf. 9th,* 1235–1247.

DAVIS A. M., TANAKA T., GROSSMAN L., LEE T. and WASSERBURG G. J. (1982) Chemical composition of HAL, an isotopically-unusual Allende inclusion. *Geochim. Cosmochim. Acta* **46,** 1627–1651.

DEINES P., NAFZIGER R. H., ULMER G. C. and WOERMANN E. (1974) Temperature-oxygen fugacity tables for selected gas mixtures in the system C-H-O at one atmosphere total pressure. *Bull. Earth Mineral Sci. Expt. Station* **88,** 1–129.

DIRSTINE R. T. and ROSA C. J. (1979) Defect structure and related thermodynamic properties of nonstoichiometric rutile (TiO_{2-x}) and Nb_2O_5 doped rutile. Part I: The defect structure of TiO_{2-x} (Rutile) and partial molar properties for oxygen solution at 1273 K. *Z. Metallkunde* **70,** 322–329.

DYAR M. D., SOLBERG T. C. and BURNS R. G. (1986) The effects of composition, oxygen fugacity, and crystal structure on the color of hibonite (abstr.). *Lunar Planet. Sci. XVII,* 194–195.

EGGLER D. H. (1983) Upper mantle oxidation state: evidence from olivine-orthopyroxene-ilmenite assemblages. *Geophys. Res. Lett.* **10,** 365–368.

EKAMBARAM V., KAWABE I., TANAKA T., DAVIS A. M. and GROSSMAN L. (1984) Chemical compositions of refractory inclusions in the Murchison C2 chondrite. *Geochim. Cosmochim. Acta* **48,** 2089–2105.

EL GORESY A. and WOERMANN E. (1977) Opaque minerals as sensitive oxygen barometers and geothermometers in lunar basalts. In *Thermodynamics in Geology* (ed. D. G. FRASER), pp. 249–277. Reidel.

EL GORESY A., NAGEL K. and RAMDOHR P. (1978) Fremdlinge and their noble relatives. *Proc. Lunar Planet. Sci. Conf. 9th*, 1279–1303.

EL GORESY A., NAGEL K. and RAMDOHR P. (1979) Spinel framboids and Fremdlinge in Allende inclusions: Possible sequential markers in the early history of the solar system. *Proc. Lunar Planet. Sci. Conf. 10th*, 833–850.

EL GORESY A., PALME H., YABUKI H., NAGEL K., HERRWERTH I. and RAMDOHR P. (1984) A calcium-aluminum-rich inclusion from the Essebi (CM2) chondrite: Evidence for captured spinel-hibonite spherules and for an ultra-refractory rimming sequence. *Geochim. Cosmochim. Acta* **48**, 2283–2298.

EL GORESY A., PALME H., SPETTEL B. and BUKOVANSKA M. (1985) Max und Moritz: Two refractory inclusions from Gorsnaja (CV3) carbonaceous chondrite (abstr.). *Lunar Planet. Sci. XVI*, 209–210.

ETSELL T. H. and FLENGAS S. N. (1970) The electrical properties of solid electrolytes. *Chem. Rev.* **70**, 339–376.

FEGLEY B. (1986) A comparison of REE and refractory metal oxidation state indicators for the solar nebula (abstr.). *Lunar Planet. Sci. XVII*, 220–221.

FEGLEY B. and KORNACKI A. S. (1984) The geochemical behavior of refractory noble metals and lithophile trace elements in refractory inclusions in carbonaceous chondrites. *Earth Planet. Sci. Lett.* **68**, 181–197.

FEGLEY B. and PALME H. (1985) Evidence for oxidizing conditions in the solar nebula from Mo and W depletions in refractory inclusions in carbonaceous chondrites. *Earth Planet. Sci. Lett.* **72**, 311–326.

FINGER L. W. (1972) The uncertainty in the calculated ferric iron content of a microprobe analysis. *Carnegie Inst. Wash. Yearb.* **71**, 600–603.

GROSSMAN L. (1972) Condensation in the primitive solar nebula. *Geochim. Cosmochim. Acta* **36**, 597–619.

GROSSMAN L. (1975) Petrology and mineral chemistry of Ca-rich inclusions in the Allende meteorite. *Geochim. Cosmochim. Acta* **39**, 433–454.

GROSSMAN L. (1980) Refractory inclusions in the Allende meteorite. *Ann. Rev. Earth Planet. Sci.* **8**, 559–608.

GROSSMAN L. and GANAPATHY R. (1976a) Trace elements in the Allende meteorite—I. Coarse-grained, Ca-rich inclusions. *Geochim. Cosmochim. Acta* **40**, 331–344.

GROSSMAN L. and GANAPATHY R. (1976a) Trace elements in the Allende meteorite—II. Fine-grained Ca-rich inclusions. *Geochim. Cosmochim. Acta* **40**, 967–977.

GROSSMAN L., GANAPATHY R. and DAVIS A. M. (1977) Trace elements in the Allende meteorite—III. Coarse-grained inclusions revisited. *Geochim. Cosmochim. Acta* **41**, 1647–1664.

HAGGERTY S. E. (1978) The Allende meteorite: Evidence for a new cosmothermometer based on Ti^{3+}/Ti^{4+}. *Nature* **276**, 221–225.

HASHIMOTO A. and WOOD J. A. (1986) Enhanced volatility of CaO in H_2O-rich gas environments as a factor in the alteration of Ca, Al-rich inclusions (abstr.). *Meteoritics* **21**, 391–392.

HASHIMOTO A., HINTON R. W., DAVIS A. M., GROSSMAN L., MAYEDA T. K. and CLAYTON R. N. (1986) A hibonite-rich Murchison inclusion with anomalous oxygen isotopic composition (abstr.). *Lunar Planet. Sci. XVII*, 317–318.

IHINGER P. and STOLPER E. (1986) The color of meteoritic hibonite: An indicator of oxygen fugacity. *Earth Planet. Sci. Lett.* **78**, 67–79.

JOHNSTON W. D. (1965) Oxidation-reduction equilibria in molten $Na_2O \cdot 2SiO_2$ glass. *J. Amer. Cer. Soc.* **48**, 184–190.

KATO K. and SAALFELD H. (1968) Verfeinerung der Kristallstruktur von $CaO \cdot 6Al_2O_3$. *N. Jb. Miner. Abh.* **109**, 192–200.

KEIL K. and FUCHS L. H. (1971) Hibonite $[Ca_2(Al, Ti)_{24}O_{38}]$ from the Leoville and Allende chondritic meteorites. *Earth Planet. Sci. Lett.* **12**, 184–190.

Kittel C. (1976) *Introduction to Solid State Physics* (5th edn.). J. Wiley & Sons, 608p.

KORNACKI A. S. and FEGLEY B. (1984) Origin of spinel-rich chondrules and inclusions in carbonaceous and ordinary chondrites. *Proc. Lunar Planet. Sci. Conf. 14th; J. Geophys. Res.* **89**, B588–B596.

KOZUL J., ULMER G. C. and HEWINS R. (1986) Intrinsic oxygen fugacities of Allende CAIs (abstr.). *Meteoritics* **21**, 425–426.

KRÖGER F. A. and VINK H. J. (1956) Relations between the concentrations of imperfections in crystalline solids. In *Solid State Physics*, Vol. 3. (eds. F. SEITZ and D. TURNBULL), pp. 307–435. Academic Press, New York.

KURAT G. (1970) Zur Genese der Ca-Al-reichen Einsclüsse im Chondriten von Lancé. *Earth Planet. Sci. Lett.* **9**, 225–231.

LELL E., KREIDL N. J. and HENSLER J. R. (1966) Radiation effects in quartz, silica and glasses. *Progr. Ceramic Sci.* **4**, 1–93.

LINDSLEY D. H. (1976) Experimental studies of oxide minerals. *Rev. Mineral.* **3**, L-61–L-88.

LIVE D., BECKETT J. R., TSAY F-D., GROSSMAN L. and STOLPER E. (1986) Ti^{3+} in synthetic hibonite: A new oxygen barometer (abstr.). *Lunar Planet. Sci. XVII*, 488–489.

LOVERING J. F., WARK D. A. and SEWELL D. K. B. (1979) Refractory oxide, titanate, niobate and silicate accessory mineralogy of some type B Ca-Al-rich inclusions in the Allende meteorite (abstr.). *Lunar Planet. Sci. X*, 745–746.

LOW W. (1968) Electron spin resonance—A tool in mineralogy and geology. *Adv. Electronics. Electron Phys.* **24**, 51–108.

MACDOUGALL J. D. (1979) Refractory-element-rich inclusions in CM meteorites. *Earth Planet. Sci. Lett.* **42**, 1–6.

MACDOUGALL J. D. (1981) Refractory spherules in the Murchison meteorite: Are they chondrules? *Geophys. Res. Lett.* **8**, 966–969.

MACPHERSON G. J. and GROSSMAN L. (1979) Melted and non-melted coarse-grained Ca-, Al-rich inclusions in Allende (abstr). *Meteoritics* **14**, 479–480.

MACPHERSON G. J. and GROSSMAN L. (1981) A once-molten, coarse-grained, Ca-rich inclusion in Allende. *Earth Planet. Sci. Lett.* **52**, 16–24.

MACPHERSON G. J. and GROSSMAN L. (1984) "Fluffy" type A Ca-, Al-rich inclusions in the Allende meteorite. *Geochim. Cosmochim. Acta* **48**, 29–46.

MACPHERSON G. J., BAR-MATHEWS M., TANAKA T., OLSEN E. and GROSSMAN L. (1983) Refractory inclusions in the Murchison meteorite. *Geochim. Cosmochim. Acta* **47**, 823–839.

MACPHERSON G. J., PAQUE J. M., STOLPER E. and GROSSMAN L. (1984) The origin and significance of reverse zoning in melilite from Allende type B inclusions. *J. Geol.* **92**, 289–305.

MASON B. and TAYLOR S. R. (1982) Inclusions in the Allende meteorite. *Smithson. Contrib. Earth Sci.* **25**, 1–30.

MURRELL M. T. and BURNETT D. S. (1987) Actinide chemistry in Allende Ca-Al-rich inclusions. *Geochim. Cosmochim. Acta* **51**, 985–999.

MYERS J. and EUGSTER H. P. (1983) The system Fe-Si-O: Oxygen buffer calibrations to 1,500 K. *Contrib. Mineral. Petrol.* **82**, 75–90.

O'REILLY D. E. and MACIVER D. S. (1962) Electron paramagnetic resonance absorption of chromia-alumina catalysts. *J. Phys. Chem.* **6**, 276–281.

PACKWOOD R. H. and BROWN J. D. (1981) A Gaussian expression to describe $\Phi(\rho z)$ curves for electron probe microanalysis. *X-Ray Spectrometry* **10**, 138–146.

PALME H. and WLOTZKA F. (1976) A metal particle from a Ca, Al-rich inclusion from the meteorite Allende, and the condensation of refractory siderophile elements. *Earth Planet. Sci. Lett.* **33**, 45–60.

PALME H., WLOTZKA F., NAGEL K. and EL GORESY A. (1982) An ultra-refractory inclusion from the Ornans carbonaceous chondrite. *Earth Planet. Sci. Lett.* **61**, 1–12.

SATO H. and HIROTSU Y. (1976) Structural characteristics and non-stoichiometry of β-alumina type compounds. *Mat. Res. Bull.* **11**, 1307–1318.

SCHMID H. and DEJONGHE L. C. (1983) Structure and non-stoichiometry of calcium aluminates. *Phil. Mag. A* **48**, 287–297.

SCHREIBER H. D. and HASKIN L. A. (1976) Chromium in basalts: Experimental determination of redox states and partitioning among synthetic silicate phases. *Proc. Lunar Sci. Conf. 7th*, 1221–1259.

SCHREIBER H. D., THANYASIRI T., LACH J. J. and LEGERE R. A. (1978) Redox equilibria of Ti, Cr, and Eu in silicate melts: reduction potentials and mutual interactions. *Phys. Chem. Glasses* **19**, 126–139.

SHANNON R. D. and PREWITT C. T. (1969) Effective ionic radii in oxides and fluorides. *Acta Cryst.* **B25**, 925–946.

SMYTH D. M. (1976) Thermodynamic characterization of ternary compounds. I. The case of negligible defect association. *J. Solid State Chem.* **16**, 73–81.

SMYTH D. M. (1977) Thermodynamic characterization of ternary compounds. II. The case of extensive defect association. *J. Solid State Chem.* **20**, 359–364.

SPENCER K. J. and LINDSLEY D. H. (1981) A solution model for coexisting iron-titanium oxides. *Amer. Mineral.* **66**, 1189–1201.

STOLPER E. (1982) Crystallization sequences of Ca-Al-rich inclusions from Allende: An experimental study. *Geochim. Cosmochim. Acta* **46**, 2159–2180.

STOLPER E. and IHINGER P. (1983) The color of meteoritic hibonite: An indicator of oxygen fugacity (abstr.). *Lunar Planet. Sci. XIV*, 749–750.

STOLPER E. and PAQUE J. M. (1986) Crystallization sequences of Ca-Al-rich inclusions from Allende: The effects of cooling rate and maximum temperature. *Geochim. Cosmochim. Acta* **50**, 1785–1806.

STOLPER E., PAQUE J. and ROSSMAN G. R. (1982) The influence of oxygen fugacity and cooling rate on the cyrstallization of Ca-Al-rich inclusions from Allende (abstr.). *Lunar Planet. Sci. XIII*, 772–773.

STOLPER E., MACPHERSON G. J., BECKETT J. R. and GROSSMAN L. (1985) Thermometry of Ca-Al-rich inclusions (abstr.). *Lunar Planet. Sci. XVI*, 827–828.

SYMONDS R. B., ROSE, W. I., REED, M. H., LICHTE, F. E. and FINNEGAN, D. L. (1987) Volatilization, transport and sublimation of metallic and non-metallic elements in high temperature gases at Merapi Volcano, Indonesia. *Geochim. Cosmochim. Acta* **51**, 2083–2101.

TANAKA T., DAVIS A. M., GROSSMAN L., LATTIMER J. M., ALLEN J. M., LEE T. and WASSERBURG G. J. (1979) Chemical study of an isotopically-unusual Allende inclusion (abstr.). *Lunar Planet. Sci. X*, 1203–1205.

TULLER H. L. (1985) Electrical conduction in ceramics: Toward improved defect interpretation. *Geophys. Mon.* **31**, 47–68.

WÄNKE H., BADDENHAUSEN H., PALME H. and SPETTEL B. (1974) On the chemistry of the Allende inclusions and their origin as high temperature condensates. *Earth Planet. Sci. Lett.* **23**, 1–7.

WARK D. A. (1980) Allende CAI 3643-A layered record of protosolar nebula condensation (abstr.). *Lunar Planet. Sci. XI*, 1202–1204.

WARK D. A. (1981) The pre-alteration compositions of Allende Ca-Al-rich condensates (abstr.). *Lunar Planet. Sci. XII*, 1148–1150.

WARK D. A. (1986) Evidence for successive episodes of condensation at high temperature in a part of the solar nebula. *Earth Planet. Sci. Lett.* **77**, 129–148.

WARK D. A. (1987) Plagioclase-rich inclusions in carbonaceous chondrite meteorites: Liquid condensates? *Geochim. Cosmochim. Acta* **51**, 221–242.

WARK D. A. and LOVERING J. F. (1982a) The nature and origin of type B1 and B2 Ca-Al-rich inclusions in the Allende meteorite. *Geochim. Cosmochim. Acta* **46**, 2581–2594.

WARK D. A. and LOVERING J. F. (1982b) Evolution of Ca-Al-rich bodies in the earliest solar system: Growth by incorporation. *Geochim. Cosmochim. Acta* **46**, 2595–2607.

WARK D. A. and WLOTZKA F. (1982) The paradoxical metal compositions in Leo-1, a type B1 Ca-Al-rich inclusion from Leoville (abstr.). *Lunar Planet. Sci. XIII*, 833–834.

WARK D. A., BOYNTON W. V., KEAYS R. R. and PALME H. (1987) Trace element and petrologic clues to the formation of forsterite-bearing Ca-Al-rich inclusions in the Allende meteorite. *Geochim. Cosmochim. Acta* **51**, 607–622.

WASSERBURG G. J., LEE T. and PAPANASTASSIOU D. A. (1977) Correlated O and Mg isotope anomalies in Allende inclusions: II. Magnesium. *Geophys. Res. Lett.* **4**, 299–302.

WOOD J. A. (1984) On the formation of meteoritic chondrules by aerodynamic drag heating in the solar nebula. *Earth Planet. Sci. Lett.* **70**, 11–26.